

FreStega: A Plug-and-Play Remedy for Imperceptibility and Capacity Enhancement in Real-World Generative Linguistic Steganography

Kaiyi Pang

Abstract—Linguistic steganography embeds secret information in seemingly innocent texts, safeguarding privacy in surveillance environments. Generative linguistic steganography leverages the probability distribution of language models (LMs) and applies steganographic algorithms to generate stego tokens, gaining attention with recent Large Language Model (LLM) advancements. To enhance security, researchers develop distribution-preserving steganographic algorithms to minimize the gap between stego sampling and LM sampling. However, the reliance on language model distributions, coupled with deviations from real-world cover texts, results in insufficient imperceptibility when facing steganalysis detectors in real-world scenarios. Moreover, LLM distributions tend to be more deterministic, resulting in reduced entropy and, consequently, lower embedding capacity. In this paper, we propose FreStega, a plug-and-play method to reconstruct the distribution of language models used for generative linguistic steganography. FreStega dynamically adjusts token probabilities from the language model at each step of stego text auto-regressive generation, leveraging both sequential and spatial dimensions. In sequential adjustment, the temperature is dynamically adjusted based on instantaneous entropy, enhancing the diversity of stego texts and boosting embedding capacity. In the spatial dimension, the distribution is aligned with guidance from the target domain corpus, closely mimicking real cover text in the target domain. By reforming the distribution, FreStega enhances the imperceptibility of stego text in practical scenarios and improves steganographic capacity by 15.41%, all without compromising the quality of the generated text. FreStega serves as a plug-and-play remedy to enhance the imperceptibility and embedding capacity of existing distribution-preserving steganography methods in real-world scenarios.

Index Terms—Linguistic Steganography, Language Model, Text Generation, Linguistic Steganalysis

I. INTRODUCTION

The widespread growth of internet surveillance has raised significant concerns about protecting personal communication privacy and safeguarding freedom of speech. Encryption is a natural choice for countering surveillance, but encrypted traffic [1] can raise suspicion among monitors. To avoid drawing attention to surveillance, it is necessary not only to encrypt the content of communications but also to hide the act of communicating itself. Steganography is the technique that embeds secret messages within seemingly innocent carriers, thereby ensuring that censors do not detect and disrupt

Kaiyi Pang is with the Tsinghua University, Beijing, 100084, China. Yongfeng Huang is also with the Zhongguancun Laboratory, Beijing, China. Tao Qi is with the State Key Laboratory of Networking and Switching Technology, Beijing University of Posts and Telecommunications, Beijing 100876, China. (taoqi.qt@gmail.com)

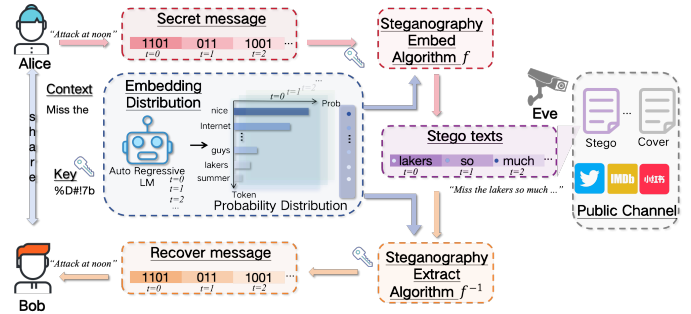


Fig. 1. Generative Linguistic Steganography Framework: Alice and Bob covertly communicate over a public channel monitored by Eve. Alice embeds secret information during the language model’s token selection process to generate stego text. Using a shared key, language model, and prompt, Bob then recovers the secret information upon receiving the stego text.

covert communication and that individuals can convey private information safely. Among the various carriers used in the information age, such as images [2] and audio [3], text naturally dominates most Internet scenarios due to its simplicity, versatility, and robustness. As a result, text steganography has garnered significant attention [4–8].

Advancements in language models have established generative linguistic steganography as a mainstream approach. This technique leverages language models to simulate the steganographic channel, utilizing the token selection process in the auto-regressive text generation to embed secret messages, as illustrated in Figure 1. State-of-the-art distribution-preserving steganography algorithms [5, 6], ensure that tokens generated through random sampling from the model are computationally indistinguishable from those generated via steganography.

Despite significant advancements, generative linguistic steganography methods still face practical challenges in the era of large language models (LLMs), notably the **de facto imperceptibility challenge** and the **low-capacity challenge**. Despite the fluency of texts generated by large language models, even the most advanced generative steganography schemes produce texts that are easily detected and blocked by automated detectors in real-world applications like social networks, often resulting in account suspensions—even before considering more advanced steganalysis techniques. **Ensuring stegotext is indistinguishable from randomly sampled language model text is not sufficient for real-world applications.** In real-world scenarios, sensors can access extensive real-world human data from the domain as cover samples to train stego detectors, a common setup in existing steganalysis

tasks [9–11].

To verify this, we tested several distribution-preserving steganography algorithms (ADG [4], METEOR [5], DISCOP [6]) with popular language models like QWEN2 [12], MISTRAL V0.3 [13], LLAMA2, and LLAMA3 [14, 15]. The token distributions and steganalysis results, shown in Figures 2 and 3, reveal that the stego texts have lower imperceptibility compared to cover texts in real-world scenarios. This occurs because existing language model distributions do not match cover texts well, and distribution-preserving methods rely entirely on these misaligned distributions. Biased language model estimations lead to a noticeable divergence between stego texts and real cover texts.

Moreover, the embedding capacity of existing generative steganography methods is constrained by the inherent distribution of the language model. Since LLMs are currently the best estimators of text channels, generative text steganography predominantly utilizes distributions generated by LLMs for steganographic sampling. **LLMs tend to produce more deterministic responses compared to smaller models [21, 22], as RLHF training often reduces the entropy of their distributions. This decrease in entropy consequently limits their embedding capacity.**

To alleviate the problems of imperceptibility and capacity in generative linguistic steganography based on unreliable language models, we propose a plug-and-play generative linguistic steganography distribution reformation method named FreStega. We reform the model’s distribution by dynamically adjusting the sharpness of the prediction distribution at each timestep (we call this **Sequential Adjustment**) and by adjusting the probability of each token using real cover text as guidance (we call this **Spatial Adjustment**). We conducted a preliminary exploration of certain methods within spatial adjustment [23] in our previous work. Building on that foundation, we further optimized the spatial adjustment method and introduced sequential adjustment. Sequential Adjustment modifies the temperature based on instantaneous entropy, reducing distribution sharpening and enhancing the diversity and embedding capacity of the stegotext. Spatial Adjustment boosts the probabilities of tokens common in the target domain while suppressing overconfidence in the language model, enabling quick adaptation to target domain distributions and enhancing imperceptibility.

Our main contributions are summarized as follows:

- **Plug-and-play and Model Agnosticism:** FreStega can be seamlessly integrated with existing generative linguistic steganography algorithms in a plug-and-play manner, including grouping-based methods such as ADG [4] and DISCOP [6], as well as AC-based methods [8, 24]. FreStega works at the decoding time of token generation, effectively aligning the generated stegotext from any auto-regressive language model with the target domain—without requiring any additional training.
- **Dual-dimensional Dynamic Distribution Adjustment:** FreStega dynamically adjusts the probability distribution of language models in both sequential and spatial dimensions. This effectively approximates the distribution of the target domain, mitigating the de facto imperceptibility

challenge of existing steganography methods caused by their heavy reliance on language model distributions when facing steganalysis in real application settings.

- **Effectiveness and Flexibility of Alignment:** Extensive experiments show that FreStega reduces distribution divergence between stego and cover texts, increasing imperceptibility against strong steganalysis detectors in the real-world scenarios while enhancing capacity without compromising linguistic quality. FreStega is also highly flexible, requiring only 100 samples to achieve effective domain alignment in Spatial Adjustment. Even without access to target domain text, Sequential Adjustment can still significantly improve the quality of stegotext.

II. GAP BETWEEN PROVABLE SECURITY AND PRACTICAL SECURITY

Existing generative linguistic steganography schemes usually utilize *language model* to approximate the distribution of the covertext channel, and design the *steganography algorithm* to be applied within this distribution [5, 25]. Autoregressive language models generate text by predicting the next token based on previous ones, ensuring coherence and context. Without steganography, tokens are randomly sampled; with steganography, the algorithm selects tokens using secret messages and keys, continuing until the sentence is complete. Significant progress has been made in developing efficient steganography algorithms, from heuristic algorithms like Bins [26] to advanced entropy-coding techniques such as Huffman Coding [27, 28], Arithmetic Coding [8] improving embedding capacity while maintaining statical security.

In recent years, several provably secure steganography schemes have been developed, theoretically ensuring that the token selection process is indistinguishable from random sampling by a polynomial-time adversary. These distribution preserving algorithms include the balanced grouping algorithm (ADG)[4], distribution copy-based distribution shifting (DISCOP)[6], one-step arithmetic coding combined with stream ciphers (METEOR)[5]. These advances have brought generative linguistic steganography closer to the security of complexity theory [25].

Despite achieving computational indistinguishability, the generated stego text still faces imperceptibility risks in real-world scenarios. These methods [5, 6] theoretically achieve the stego texts generated are indistinguishable from texts generated by language model random sampling. However, in practice, particularly on social networks, using generated texts from language models as cover texts is an unrealistic assumption. Human-generated content remains dominant on mainstream platforms, and many social networks employ bot detection mechanisms (e.g., Reddit, XHS). As shown in Figures 2 and 3, stego texts generated by state-of-the-art distribution-preserving algorithms [5, 6] exhibit an apparent discrepancy from real-world cover texts (e.g., real comments on IMDB) in both word frequency distribution and steganalysis performance. The steganalysis follows the mainstream paradigm [9–11, 17, 29], focusing on distinguishing real cover texts in the target domain from stego texts.

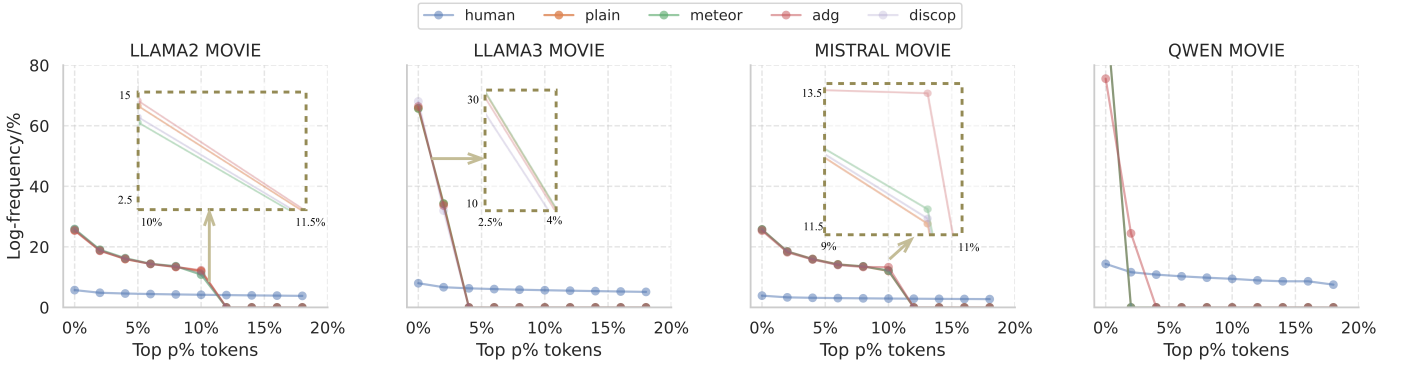


Fig. 2. Word frequency distribution comparison between text generated by state-of-the-art distribution-preserving algorithms (METEOR [5], ADG [4], DISCOP [6]), Random Sampling (RS), and cover text on the IMDB [16] using various LLMs (In each model scenario, the tokenizer corresponding to that specific model is used for tokenization and frequency statistics. Therefore, the distribution of the same human corpus may vary slightly after tokenization by different models).

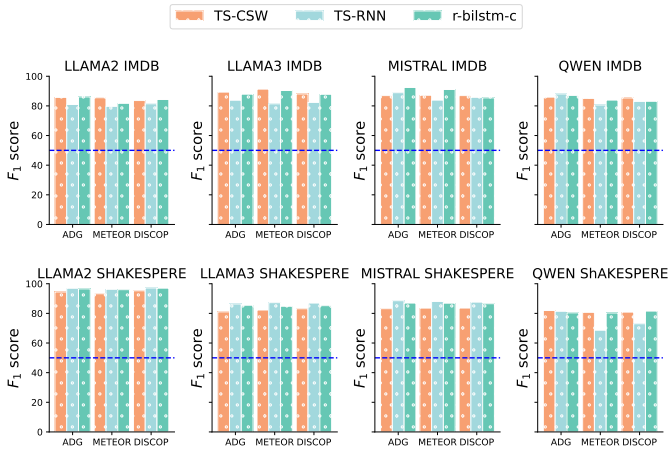


Fig. 3. F1 classification scores of state-of-the-art steganography methods (ADG [4], METEOR [5], DISCOP [6]) against classic steganalysis classifiers (TS-CSW [17], TS-RNN [18], and R-BiLSTM-C [19]) on the IMDB [16] and SHAKESPEARE [20] in real-world scenarios.

The gap is mainly caused by the mismatch between the distribution used for steganography and the real-world cover text distribution. This issue is especially evident with LLMs, which, even after fine-tuning or using few-shot examples, struggle to fully align with cover text distributions in practical applications. Many studies [30–33] have identified biases in language models’ predictive distributions compared to human language. These models tend to overestimate frequently seen tokens and underestimate rare ones, leading to inflated common word frequencies and suppressed rare ones.

Distribution-preserving steganography algorithms such as DISCOP [6] and METEOR [5], rely on the steganography sampling distribution to perfectly match the language model distribution. For example, DISCOP requires cyclic shifts in the language model distribution, and METEOR uses one-step arithmetic coding based on exact distributions, both requiring precise reference to the language model distribution. The consistency between the steganographic sampling distribution and the language model’s original predictive distribution is a fundamental requirement for security considerations. Therefore, if the predictive distribution of a language model significantly

deviates from the real-world cover text distribution, it may pose substantial security risks to provable secure steganography schemes.

In terms of capacity, existing distribution-preserving schemes rely entirely on the language model’s distribution, with the upper limit determined by its entropy. Increasing the temperature is a common approach to enhance capacity. However, rigid temperature adjustments can degrade text quality and increase detectability by steganalysis.

In summary, **existing distribution-preserving algorithms are heavily dependent on the language model’s distribution. However, current language model distributions still struggle to meet the practical demands of steganography in terms of imperceptibility and capacity.** Furthermore, existing steganography frameworks often neglect to describe this gap. Existing complexity-based steganographic algorithms focus on ensuring that steganographic embedding and random sampling under a given generative model are computationally indistinguishable. However, this descriptive framework is incomplete for practical applications, as it relies on an idealized assumption of the model-based steganographic channel and fails to adequately account for real-world cover channels.

III. METHOD

A. Preliminary

In practical applications, the text steganography process can be formally modeled as follows. The sender, Alice, and the receiver, Bob, share a secret key \mathcal{K} , language model \mathcal{M} , and historical context \mathcal{H} . They can use \mathcal{K} as the seed for the pseudorandom generator (PRG) to generate a sequence of pseudorandom bits used in the steganography algorithms. Alice encodes the secret messages $B = \{b_0, b_1, \dots, b_n\}, b_i \in \{0, 1\}$ into the stego text T using the language model \mathcal{M} , based on historical context \mathcal{H} within the steganography application environment \mathcal{E} . In practice, both the sender and receiver can access a sampled dataset from the target environment \mathcal{E} , denoted as $I_{\mathcal{E}}$ —a finite collection of textual examples representative of the domain. We model $I_{\mathcal{E}}$ as the set $\{e_1, e_2, \dots, e_q\}$, where each e_i represents an individual sentence sampled from \mathcal{E} . The distribution of $I_{\mathcal{E}}$ serves as an approximation of the

broader distribution of \mathcal{E} , a foundational assumption in statistical language processing [34]. Bob decodes the stego text $T = \{x_0, x_1, \dots, x_m\}$ (where each x_i is a token from the vocabulary of \mathcal{M}) and recovers the secret messages B using the shared key \mathcal{K} , language model prefix prompt \mathcal{H} , and language model \mathcal{M} within environment \mathcal{E} .

$$\mathbf{Encode}(\mathcal{K}, \mathcal{M}, \mathcal{H}, I_{\mathcal{E}}, B) \xrightarrow{\text{generate}} T, \quad (1)$$

$$\mathbf{Decode}(\mathcal{K}, \mathcal{M}, \mathcal{H}, I_{\mathcal{E}}, T) \xrightarrow{\text{recover}} B. \quad (2)$$

The steganography system should meet the requirement of *correctness*, ensuring that the secret message B can be accurately recovered after being embedded and extracted from the stegotexts T :

$$\mathbf{Decode}(\mathcal{K}, \mathcal{M}, \mathcal{H}, I_{\mathcal{E}}, \mathbf{Encode}(\mathcal{K}, \mathcal{M}, \mathcal{H}, I_{\mathcal{E}}, B)) = B. \quad (3)$$

More specifically, we use the language model \mathcal{M} to mimic the cover channel of environment \mathcal{E} and embed secret message B in the output tokens of \mathcal{M} . We use the most widely adopted auto-regressive language models for our analysis here. An auto-regressive language model \mathcal{M} utilizes its own output to inform the subsequent prediction. The prediction process can be formalized as:

$$\mathcal{M}(x_0, x_1, \dots, x_{i-1}, \mathcal{H}) \xrightarrow{\text{predict}} P(x_i | x_0, x_1, \dots, x_{i-1}, \mathcal{H}), \quad (4)$$

The probability of the entire sequence $T = \{x_0, x_1, \dots, x_m\}$ conditioned on prior context \mathcal{H} can be factorized as:

$$P(T | \mathcal{H}) = P(x_0 | \mathcal{H}) \cdot P(x_1 | x_0, \mathcal{H}) \cdot \dots \cdot P(x_m | x_{<m}, \mathcal{H}), \quad (5)$$

$$P(T | \mathcal{H}) = \prod_{t=0}^m P(x_t | x_{<t}, \mathcal{H}). \quad (6)$$

Typically, a normal language model samples x_t randomly from the immediate conditional distribution $P(x_t | x_{<t}, \mathcal{H})$ and concatenates it to the history $x_{<t} | x_t: x_t \sim P(x_t | x_{<t}, \mathcal{H})$. The model then predicts the distribution for the next token, $P(x_{t+1} | x_{<t+1}, \mathcal{H})$, continuing this process until the sentence reaches the maximum length or an early stopping condition is met. In the process of generative linguistic steganography, we use steganography algorithms f [5, 6] to replace random sampling in the auto-regressive process of text generation. These algorithms map tokens to binary secret bits based on $P(x_t | x_{<t}, \mathcal{H})$ at each time step, thereby determining the next token x_t :

$$x_t = f(B_t, \mathcal{K}, P(x_t | x_{<t}, \mathcal{H})), \quad (7)$$

where B_t represents the binary secret bits to be embedded at time step t , which is a piece of B . f maps the binary secret bits B_t to a token x_t . The process then continues as in a standard autoregressive language model, where the generated x_t is concatenated to the historical information and used as a condition for the next step $t+1$, until the stego sentence T is fully generated. Alice then sends the generated stego text T in a suitable way through the monitored environment. \mathcal{E} can be any uncontrolled channel capable of carrying textual content, such as various social media platforms like Twitter, XHS, etc.

Bob, upon receiving the stego text T within \mathcal{E} , uses the shared key \mathcal{K} , the model \mathcal{M} , and the prefix prompt \mathcal{H} to

reconstruct the probability distribution $P(x_t | x_{<t}, \mathcal{H})$ at each time step. Using the steganography extraction algorithm f^{-1} , Bob recovers the secret message B_t :

$$B_t = f^{-1}(x_t, \mathcal{K}, P(x_t | x_{<t}, \mathcal{H})). \quad (8)$$

By applying this process to all received tokens, Bob reconstructs the entire secret message B .

It is obvious that Alice and Bob aim for the stego text to blend seamlessly into \mathcal{E} . Specifically, the objective is for the language model distribution $P(x_t | x_{<t}, \mathcal{H})$ used for steganographic sampling to closely approximate the actual distribution of the environment \mathcal{E} , even when the true distribution of \mathcal{E} is unavailable. The surveillant, Eve, continuously monitors the communication between Alice and Bob. Here, we assume that Eve is a passive adversary who does not actively alter the text sent by Alice. In accordance with the standard practices in contemporary text steganalysis methods, Eve designs a detector to perform classification and determine whether the transmitted text T is stego or cover. If T is discriminated as stego, the communication channel between Alice and Bob will be cut off. The text T is regarded as stego if $p(S | D(T, \mathcal{E})) > p(C | D(T, \mathcal{E}))$, where S and C represent stego and cover categories, respectively. $p(\cdot)$ denotes the learned posterior probability distribution, and D represents the learned feature extractor of the stego detector. In real-world applications, the steganalyst has ample information about the environment \mathcal{E} . Simply identifying whether a text exhibits the characteristics of the target application domain \mathcal{E} can effectively expose and block many stego texts, even those generated by sophisticated steganography methods. The most common paradigm for text steganalysis [10, 11, 17, 18] involves collecting a batch of stego texts and a batch of real cover texts within a specific environment. Detectors then focus on distinguishing features for classification. Additionally, contextual information from the application environment (e.g., social networks) can be utilized to further improve detection [9].

B. Narrowing the Gap Toward Real-World Scenarios

When applying generative text steganography schemes in real-world scenarios, a fundamental consideration is that the generated stego texts should seamlessly fit into the environment. Specifically, the stego sampling distribution p_S should closely resemble the target domain's cover distribution $p_{\mathcal{E}}$: $p_S = \arg \min_{p_S} D_{KL}(p_{\mathcal{E}} \| p_S)$. We denote the original language model distribution $p_{\mathcal{M}}$, which represents the random sampling process of the language model \mathcal{M} . The embedding process introduces noise ϵ , leading to a new distribution $p_S = p_{\mathcal{M}} + \epsilon$. While KL divergence does not satisfy the triangle inequality, for small ϵ , we can approximate it as:

$$\begin{aligned} D_{KL}(p_{\mathcal{E}} \| p_S) &= D_{KL}(p_{\mathcal{E}} \| p_{\mathcal{M}} + \epsilon) \\ &\approx D_{KL}(p_{\mathcal{E}} \| p_{\mathcal{M}}) + \epsilon \cdot \nabla D_{KL}(p_S \| p_{\mathcal{M}}) + \mathcal{O}(\epsilon^2). \end{aligned} \quad (9)$$

For an ideal statistically secure distribution-preserving steganography algorithm, $\epsilon = 0$ is considered theoretically achievable, meaning that $D_{KL}(p_S \| p_{\mathcal{M}}) = 0$, and the quality of the stego text is primarily determined by $p_{\mathcal{M}}$. But this is

not the end to pursue higher imperceptibility in real-world scenarios. Despite the great advancements that have been made to decrease $D_{KL}(p_S||p_M)$. This also highlights the issue of heavy dependence on the language model distribution that we discussed earlier. The security and quality of the stego text totally depend on $D_{KL}(p_E||p_M)$. Narrowing the gap between the language model distribution p_M and the target domain text distribution p_E significantly enhances the imperceptibility of current steganography schemes, including both distribution-preserving and non-distribution-preserving algorithms. The noise introduced by non-distribution-preserving algorithms is further analyzed in the Appendix VI-A.

There are two main intuitive approaches to generating stego text that align with the characteristics of the target domain \mathcal{E} .

The first approach is to **fine-tune** or **refactor** \mathcal{M} to \mathcal{M}_E [35, 36] using a large corpus I_E , allowing the model to learn domain-specific characteristics during targeted training. The second approach is to **optimize prompts**, including prompt-tuning or instruction-guiding methods [37, 38], which involve finding a suitable prompt \mathcal{H} or its soft embedding. This is more effective for large models with strong instruction-following capabilities [39, 40], enabling them to generate text that reflects the style of \mathcal{E} .

Fine-tuning or refactoring \mathcal{M} to align with a target steganography domain is a straightforward approach [35]. This process adjusts the model’s parameters θ to minimize the loss \mathcal{L} on the target dataset I_E , learning the characteristics of \mathcal{E} :

$$\theta_E = \arg \min_{\theta} \mathbb{E}_{(x,y) \sim I_E} [\mathcal{L}(y, \mathcal{M}(x; \theta))], \quad (10)$$

where θ_E are the fine-tuned parameters, $\mathcal{M}(x; \theta)$ is the model’s prediction, and I_E is the dataset from \mathcal{E} . Aligning a model with a target domain’s language style through fine-tuning is challenging. Fine-tuning large-scale models or pretraining from scratch is computationally expensive, even with parameter-efficient methods like LoRA [41]. Preference alignment methods [42] often require extensive human-labeled data for reinforcement learning, making them difficult to apply for unsupervised adaptation to target domain styles. Additionally, obtaining effective supervised signals for open-generation tasks in steganography is challenging, as most research focuses on discrimination tasks and fine-tuning models with knowledge-rich data, resulting in AI-assistant-style, low-entropy responses. Steganography, however, seeks to mimic the natural cover style of the target domain to avoid detection. Texts in typical steganography application domains, such as social networks, often lack rich knowledge, are low quality, and sometimes ungrammatical, making them unsuitable as training data.

In the **prompt-based approach**, a carefully designed prompt \mathcal{H}_E is added to the input sequence to guide the language model in generating text that matches the style of \mathcal{E} : $p_M = p(x_t|x_{<t}, \mathcal{H}_E)$. Finding effective prompts to align with \mathcal{E} ’s characteristics is still challenging. Direct instructions work well for large language models trained to follow commands but often fail to fully capture the target domain’s style. Identifying the optimal prompt often requires complex training. Existing prompt-tuning methods optimize a continuous prefix to extract task-specific embeddings from models like BERT [43],

but these methods are not ideal for implicit linguistic style alignment. Some approaches [44, 45] use control tokens for explicit preferences, but they lack scalability and adaptability, making them unsuitable for the implicit alignment needed in steganography. Optimizing prompts is a complex topic and not the primary focus of our method. It is worth noting that the FreStega is applicable regardless of whether the model has been fine-tuned for specific tasks or guided by prompts. Our approach enhances alignment, improving upon these imperfect methods to better match the target application domain.

Our method works during the **decoding stage** of language models, improving the distribution $P(x_t|x_{<t}, \mathcal{H}_E) \leftarrow M_E$ of both fine-tuned models and prompt-guided models. In other words, **our method is compatible with both fine-tuning and prompt-based approaches**. The compatibility analysis is provided in Section IV-E1. Most existing controllable text generation methods [46–48] at the decoding stage focus on explicit semantic attribute control and often require additional specially designed classifiers [46, 48]. To our knowledge, there have been only two prior attempts to apply decoding-phase methods for stegotext generation. One, by [49], builds on PPLM [46], but this approach requires dimensional alignment between the classifier and the language model, making it difficult to scale to current LLMs. Another preliminary attempt [23] adjusts the softmax to infuse a certain target-domain style into the generated stegotext. However, this method overlooks capacity issues from LLMs’ low entropy and fails to suppress their inherent AI style.

C. Overview

Our objective is twofold: to mitigate the intrinsic bias in language models, thereby producing stego text with greater diversity and a style more akin to cover texts in the application domain, and to increase the entropy of generated text while preserving the linguistic quality of generated stego texts.

We adjust the language model distribution p_M for better steganography by addressing two key aspects: aligning it more closely with p_E to enhance practical imperceptibility, and mitigating the sharpening effect to slightly increase entropy while preserving linguistic quality, thereby boosting embedding capacity.

For a text sequence $\mathbf{x} = x_0, x_1, \dots, x_{N-1}$, where each $x_i = w_k \in \mathcal{V}$ is a token from the model tokenizer vocabulary. The auto-regressive language model used as the base model for generative steganography models the distribution of a sentence \mathbf{x} as a product of conditional probabilities $p(x_i|\mathbf{x}_{0:i-1})$ using the chain rule: $p(\mathbf{x}) = \prod_{i=0}^{N-1} p(x_i|\mathbf{x}_{0:i-1})$.

The probability of token w_k appended at the t -th position of sentence \mathbf{x} is computed as Equation 11:

$$\hat{p}(x_t = w_k|\mathbf{x}_{0:t-1}) = \frac{e^{\mathbf{h}^t \cdot \mathbf{o}_k^t}}{\sum_{w_i \in \mathcal{V}} \{e^{\mathbf{h}^t \cdot \mathbf{o}_i^t}\}}, \quad (11)$$

where \mathbf{o}_k^t and \mathbf{h}^t denote the output layer and the hidden states of LM at t -th step in the generation process, respectively.

Our method modifies the conditional probability distribution $p(x_t|\mathbf{x}_{<t})$ across both sequential and spatial dimensions to approximate target domain cover distribution, as shown in

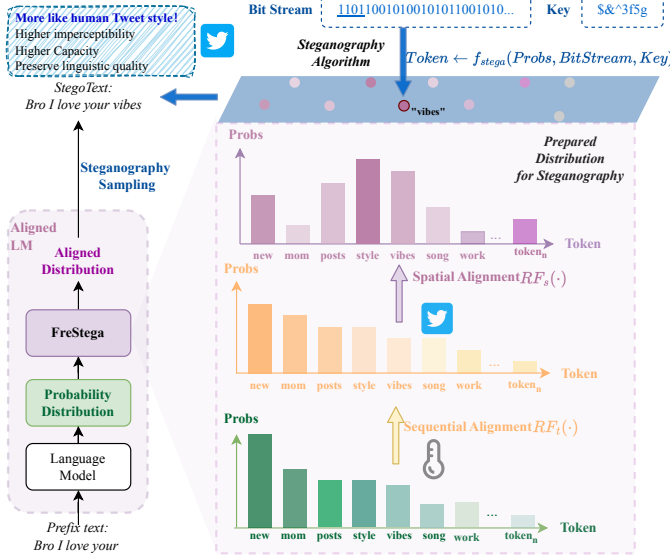


Fig. 4. Overview of FreStega: We first adjust the temperature at each time step based on the instantaneous entropy in the sequential dimension. Then, we refine the language model’s distribution in the spatial dimension, aligning it with the target domain’s cover distribution.

Figure 4. FreStega adjusts the original distribution p_M to a distribution better suited for steganography sampling algorithms. The steganography algorithm does not require any modifications; it determines the next token based on the key and secret information within the new distribution.

In the sequential dimension, we make a balanced exploration of the model’s output, ensuring a more diverse and natural flow of language. By incorporating this dynamic temperature regulation in every time step, we aim to increase embedding capacity and creativity in the generated stegotext while preserving fluency.

In the spatial dimension, we align the language model’s distribution with the token frequency distribution of the target cover corpus. It’s worth noting that we use the token frequency distribution of the language model in our experiments because the token frequency is the most direct marginal distribution of texts. In fact, our method can be applied to other marginal distributions, such as sentiment or topic.

As a result, the language model is more adapted to generating texts that closely resemble those in the target domain cover text. The pseudocode of the overall method is shown in Algorithm 1. We elaborate on the sequential alignment and spatial alignment in Algorithm 1 in detail in III-D and III-E, respectively.

D. Sequential Dimension

Our adjustments in the sequential dimension serve two purposes: first, to increase entropy while maintaining generation quality to enhance embedding capacity; and second, to counteract the model’s sharpening effect [30], a tendency where the model becomes overly confident in its predictions, which can reduce the diversity and creativity of the generated stego text.

Algorithm 1 Probability distribution reformation and stegotext generation

Input: target domain corpus \mathcal{D} ; model original generated corpus \mathcal{M} ; language model LM ; tokenizer T ; token vocabulary \mathcal{V} ; input text $\mathbf{x}_{0:t-1}$, steganography algorithm f ; shared key \mathcal{K} ; Secret bits B .

Output: output text \mathbf{x} .

- 1: $\cdot \cdot \cdot$ Initial frequencies
- 2: **for** $v \in \mathcal{V}$ **do**
- 3: $D_{freq}(v) \leftarrow \frac{Count^{T(\mathcal{D})}(v)}{\#T(\mathcal{D})}$
- 4: $M_{freq}(v) \leftarrow \frac{Count^{T(\mathcal{M})}(v)}{\#T(\mathcal{M})}$
- 5: **end for**
- 6: **while** $x_{t-1} \neq \text{EOS}$ **do**
- 7: $\cdot \cdot \cdot$ Sequential alignment
- 8: $\mathbf{L} \leftarrow LM(\mathbf{x}_{0:t-1})$
- 9: $\mathbf{P} \leftarrow \frac{e^{\mathbf{L}}}{\text{sum}(e^{\mathbf{L}})}$
- 10: $E_{t-1} \leftarrow -\mathbf{P}^T \cdot \log(\mathbf{P})$
- 11: $TP_{t-1} \leftarrow Temp(E_{t-1})$
- 12: $\mathbf{L}_{RF} \leftarrow RF_t(\mathbf{L}, TP_{t-1})$
- 13: $\cdot \cdot \cdot$ Spatial alignment
- 14: $\mathbf{L}_{RF} \leftarrow RF_s(\mathbf{L}_{RF}, D_{freq}(v), M_{freq}(v))$
- 15: $\mathbf{P}_{RF} \leftarrow \frac{e^{\mathbf{L}_{RF}}}{\text{sum}(e^{\mathbf{L}_{RF}})}$
- 16: $\cdot \cdot \cdot$ Stego sampling
- 17: $x_t = w_j \leftarrow f(B_i, \mathcal{K}, \mathbf{P}_{RF})$
- 18: $t \leftarrow t + 1$
- 19: **end while**
- 20: **return** output stegotext \mathbf{x}

We dynamically adjust the temperature at each time step t based on the instantaneous entropy E_t of the model:

$$E_t = - \sum_{k \in \mathcal{V}} p(w_k | \mathbf{x}_{0:t-1}) \cdot \log[p(w_k | \mathbf{x}_{0:t-1})]. \quad (12)$$

By dynamically adjusting the temperature, which influences the certainty of the model’s selections, we preserve the original token sequence predicted by the model while reducing its bias toward overly confident patterns. This strategy enhances the model’s ability to generate diverse and varied stego text, better capturing the natural unpredictability and richness of human language. The temperature TP_t at time step t is adjusted using the temperature function $Temp(\cdot)$:

$$TP_t = Temp(E_t) = 1 + \theta * \log_2(1 + c * E_t), \quad (13)$$

where TP_t is the adjusted temperature at time step t , c is the factor controlling the adjustment strength, θ is a scaling factor, which we typically fix at 0.01, and the base value 1 represents the default temperature typically provided by LLMs from HuggingFace, which can be determined by user settings. We chose a logarithmic function because the log function $\log(x)$ naturally counteracts the exponential nature of the softmax (i.e., the $e^{(x)}$ term), making it inherently effective at mitigating distribution sharpening in language models: when the entropy is low, the temperature increases rapidly; when the entropy is high, the temperature increases slowly. Given that E_t ranges within $[0, \log_2(\text{Tokenizer.VocabSize})]$, the adjustment range of TP_t is bounded within $[0, 0.01 \cdot$

$\log_2(1+c\cdot\log_2(\text{Tokenizer.VocabSize}))$], representing a modest smoothing effect. This design aligns with our primary goal of increasing the entropy of the generated stegotext — and thus enhancing steganographic capacity — while preserving linguistic quality. Other forms of entropy-driven dynamic temperature adjustment functions, as long as they maintain a positive first derivative and negative second derivative within $[0, \log_2(\text{VocabSize})]$, can also be employed as alternative strategies in our sequential adjustment framework to mitigate distribution sharpening.

The probability of each token will be readjusted by the sequential probability distribution reform function RF_t .

$$L_{RF_t}(x_t = w_k | \mathbf{x}_{0:t-1}) = \frac{\mathbf{h}^t \cdot \mathbf{o}_k^t}{TP_t}. \quad (14)$$

$L_{RF_t}(x_t = w_k | \mathbf{x}_{0:t-1})$ is the logits of token w_k after sequential reformation RF_t in the time step t .

E. Spatial Dimension

Several works [30, 31] have mentioned that LMs have a distorted preference for the next token prediction in text generation. The estimation of language distribution from the Bayesian perspective actually is:

$$\hat{p}(x_t = w_k | \mathbf{x}_{0:t-1}) = \frac{p(\mathbf{x}_{0:t-1} | x_t = w_k) p(x_t = w_k)}{p(\mathbf{x}_{0:t-1})} \quad (15)$$

$$= \begin{cases} \frac{p(\mathbf{x}_{0:t-1} | x_t = w_k)}{p(\mathbf{x}_{0:t-1})} \frac{n'_k}{\sum_i |\mathcal{V}| n'_i}, & \text{in generated text,} \\ \frac{p(\mathbf{x}_{0:t-1} | x_t = w_k)}{p(\mathbf{x}_{0:t-1})} \frac{n_k}{\sum_i |\mathcal{V}| n_i}, & \text{in training corpus.} \end{cases}$$

where n_k , n_i ; n'_k , n'_i denote the token k 's and any i 's frequency in the training corpus and generated text, respectively.

Tokens with the highest frequency in the training corpus appear even more frequently in the generated texts ($n_k > n'_k$), while rare tokens become even rarer ($n_k < n'_k$).

The intuitive idea behind the Spatial Adjustment function is to weaken the model's own bias towards certain tokens as much as possible and to closely approximate the distribution of tokens in the target cover corpus.

For the purposes of plug-and-play alignment with a target domain, we selected token frequency as our guiding signal because it represents the most intuitive and readily obtainable marginal distribution of text. From a statistical perspective, token frequency distributions in a corpus are widely regarded as empirical probability distributions of the language—a view supported by both statistical natural language processing [34] and information theory [50]. Such distributions offer a clear and efficient proxy for capturing textual characteristics and can be seamlessly incorporated into the decoding process of a language model.

To revise the biased LMs distribution, we apply a spatial distribution reform function RF_s to reform the logits of a token w_k . The reformed logits L_{RF_s} are shown in the following Equation 16:

$$L_{RF_s}(w_k | \mathbf{x}_{0:t-1}) = \mathcal{F}(w_k; \mathcal{D}, \mathcal{M}) \cdot L_{RF_t}(\cdot), \quad (16)$$

where $L_{RF_t}(\cdot)$ denotes the result of sequential dimension reformation. $\mathcal{F}(w_k; \mathcal{D}; \mathcal{M})$ denotes the function calculated by the n -gram frequency of w_k in target corpus \mathcal{D} and in origin model random sampling generated texts corpus \mathcal{M} , which is shown in Equation 17:

$$\mathcal{F}(\mathbf{w}; \mathcal{D}, \mathcal{M}) = \log(2 + [\frac{f(\mathbf{w}; \mathcal{D})}{f(\mathbf{w}; \mathcal{M})}]^\alpha), \quad (17)$$

where $f(\mathbf{w}; \mathcal{D})$ is the static n -gram frequency of sequence \mathbf{w} in the targeted corpus \mathcal{D} , $f(\mathbf{w}; \mathcal{M})$ is the static n -gram frequency of sequence $\mathbf{w} | \mathbf{x}_{t-n:t-1}$ in the origin LM generated texts corpus \mathcal{M} , and hyper-parameter α controls the intensity of spatial dimension reformation.

The frequency adjustment function $\mathcal{F}(w_k; \mathcal{D}; \mathcal{M})$ makes its frequency distribution closer to that of target domain cover corpus \mathcal{D} , diminishing the dominance of the frequency distribution inherent to the original model-generated text corpus \mathcal{M} . In this way, we force language models to output a distribution that more closely resembles the target domain cover texts. The reformed probability is

$$p_{RF_s}(w_k | \mathbf{x}_{0:t-1}) = \frac{L_{RF_s}(w_k | \mathbf{x}_{0:t-1})}{\sum_{w_i \in \mathcal{V}} L_{RF_s}(w_i | \mathbf{x}_{0:t-1})}. \quad (18)$$

IV. EXPERIMENTS

A. Experiment Setup

FreStega, as a plug-and-play module, can seamlessly adapt to any language model for next-token prediction, any steganographic sampling algorithm, and any target linguistic style. In our main experiment, we tested FreStega with four large language models, various steganography algorithms, and three datasets representing distinct human styles¹.

1) *Baselines*: FreStega requires no additional training modules like classifiers. Existing attribute-controlled text generation methods are hard to apply directly to steganography and often need carefully designed training modules, making comparison with FreStega difficult. We evaluated FreStega using the random sampling decoding method (viewed as the ideal steganography algorithm) and four state-of-the-art generative steganography algorithms: AC [8], ADG [4], METEOR [5], and DISCOP [6]. The performance of these representative methods was also assessed as baselines. These generative steganography methods map the token probabilities distribution into secret bits to determine the next generated token. AC [8] uses arithmetic coding to map the token probability distribution of the language model onto the real interval $[0, 1]$. The secret bitstream is then mapped to a real number within this interval to determine the next token. ADG [4] dynamically groups token probabilities to form a complete binary tree that maps to the secret information as evenly as possible. METEOR [5] requires the sender and receiver to share a secret key. In each step of embedding the language model token probability distribution, similar to one-step AC, the secret information is re-encrypted. METEOR is the first implementation of a provably secure linguistic steganography method. Ding et al.

¹Our code and data are available at <https://github.com/anonymousP0722/FreStega>

[6] proposed DISCOP, which uses copies of the distribution to embed secret messages. When the random numbers $r \in [0, 1)$, $r + \frac{1}{2^n} \bmod 1$, $r + \frac{2}{2^n} \bmod 1$, ..., $r + \frac{2^n - 1}{2^n} \bmod 1$ each point to different tokens, the embedding capacity is n bits.

2) *Datasets*: We selected three datasets with distinct human characteristics that are challenging for models to mimic: IMDB [16], XHS [51], and Shakespeare². IMDB and Shakespeare are English datasets, while XHS is in Chinese. IMDB and XHS represent popular online social platforms known for their informal, fragmented language, making them common scenarios for covert text communication. The Shakespeare dataset is used to simulate situations where stego text needs to match the sender’s usual style. These datasets, due to their informality and low knowledge intensity, are typically underrepresented in LLM pre-training. The corpus statistics are provided in the Appendix VI-B. In the main experiment, we used the entire target domain for alignment and explored the effect of varying the amount of target domain data in subsequent analyses.

3) *Models*: We evaluate FreStega using four large language models (MISTRAL v0.3 [13], QWEN2 [12], LLAMA2 [14] and LLAMA3 [15]). We utilize MISTRAL v0.3 [13], QWEN2 [12], LLAMA2 [14] and LLAMA3 [15] as the base models in English dataset, with model scales of 7B, 7B, 7B and 8B, respectively. Due to the fact that the XHS dataset is entirely in Chinese, We utilized QWEN2 7B [12] and CHATGLM3 6B [52], which were primarily trained on Chinese data. Since large language models with around 7 billion parameters have already demonstrated strong instruction understanding capabilities, we conducted all our tests in a zero-shot scenario. The prompts we used are detailed in the Appendix VI-B. These prompts are loaded into the function `apply_chat_template` and then become the input of LLMs. For each test, we let the models generate 10,000 samples with $\text{top-}p = 1.0$, $\text{base temperature} = 1.0$. All our experiments were conducted on $2 \times$ NVIDIA A5000 GPUs (32GB RAM) and $24 \times$ Intel Xeon w5-3423 CPUs.

B. Metrics

We primarily evaluate the quality of stego text based on three criteria: **linguistic quality** (including *perplexity* and *diversity*), **capacity** (including *entropy* and *embedding rate*), and **domain statistical imperceptibility** (including *MAUVE* [53] and *steganalysis F1 scores*).

1) *Linguistic Quality*: Although perplexity (PPL) does not fully capture the quality of generated text, it can to some extent reflect its fluency. A lower PPL can be considered as smoother generated text. We use Qwen2-7B as the evaluator to calculate PPL in the experiments. $PPL = \exp\left(-\frac{1}{N} \sum_{i=1}^N \log p(x_i | \mathbf{x}_{1:i-1})\right)$.

As for text diversity, we used the $distinct_n$ metric. This metric needs to find the unique pieces of tokens in the text and calculate their ratio. $distinct_n = \frac{\text{count}(\text{unique } n\text{-grams})}{\text{count}(n\text{-grams})}$. In the main experiments, we typically use $distinct_3$,

2) *Capacity*: Entropy measures the richness of information in a sentence, with higher entropy indicating more meaningful content. It also represents the upper limit of generative linguistic steganographic capacity [22].

$$\text{entropy} = \sum_{i=1}^N \sum_{j=1}^{|\mathcal{V}|} p_i(w_j | \mathbf{x}_{1:i-1}) \log p_i(w_j | \mathbf{x}_{1:i-1}). \quad (19)$$

In our experiments, we use the average entropy per token as the measurement, defined as: $\frac{\text{entropy}}{\text{token}} = \frac{1}{N} \sum_{i=1}^N \sum_{j=1}^{|\mathcal{V}|} p_i(w_j | \mathbf{x}_{1:i-1}) \log p_i(w_j | \mathbf{x}_{1:i-1})$.

The Embedding Rate (ER) quantifies the payload of stegotext by measuring the average number of embedded bits per token. A higher ER indicates a greater relative embedding capacity. The ER is calculated using the formula: $ER = \frac{L}{N_t}$, where L is the length of the embedded message, and N_t is the number of tokens in the stegotext. It is important to note that, unlike traditional steganography methods where the embedding rate is predefined, the embedding rate in state-of-the-art distribution-preserving steganography algorithms is determined dynamically based on the distribution.

3) *Domain Statistical Imperceptibility*: The main goal of steganography is to conceal a secret message so that it appears as an innocent carrier. We mainly measure the imperceptibility of stegotext from two perspectives: the degree of similarity to the distribution of real covertext in the target domain and the ability to resist detection by steganalysis. In addition, we analyzed whether FreStega can enhance resistance to AIGT detection, a step that is typically performed before content is published on real-world online platforms.

We employ the MAUVE [53] metric to evaluate how closely the probability distribution of the generated stegotext aligns with that of the target domain human text, estimated by Monte Carlo methods:

$$\text{MAUVE}(D_{\text{stego}}, D_{\text{cover}}) = \text{AUC}(C(D_{\text{stego}}, D_{\text{cover}})), \quad (20)$$

$$C(D_{\text{stego}}, D_{\text{cover}}) = \{(\exp(-cKL(Q|R_\lambda)), \exp(-cKL(P|R_\lambda))) | R_\lambda = \lambda D_{\text{stego}} + (1 - \lambda) D_{\text{cover}}, \lambda \in (0, 1)\}, \quad (21)$$

Here, $\text{AUC}(x)$ denotes the area under curve x , and $C(D_{\text{stego}}, D_{\text{cover}})$ represents the divergence curve between D_{stego} and D_{cover} . This curve provides more detailed insights than the standard Kullback-Leibler divergence, $KL(\cdot | \cdot)$. The parameter $c > 0$ is used for scaling.

We also utilized three classic steganalysis models to assess the imperceptibility of stegotexts: TS-CSW [17], TS-RNN [18], and R-BiLSTM-C [54] based on pre-trained BERT [55]. We trained these detectors with 1,000 samples of generated stegotexts and the target domain human corpus at every single test. The datasets for training, validation, and testing were split in a ratio of 3:1:1. The learning rate was set to $1e-4$, and training was conducted for three epochs. After repeating this process three times, we evaluated the average F1 score of the test set as the steganalysis F1 score.

²<https://hf.com/datasets/ayaan04/shakespeare-text>

TABLE I
IMDB MAIN RESULT. "W/O" INDICATES MODELS WITHOUT FREStEGA, WHILE "W/" INDICATES MODELS WITH FREStEGA.

Model	Algorithm	Linguistics		Capacity		Domain Statistical Imperceptibility			
		Div.↑	PPL↓	Entro./token↑	ER ↑	MAU.↑	CSW-F1↓	RNN-F1↓	r-bilstm-c-F1↓
LLAMA2 [14]	RS w/o	0.12	3.03	0.80	/	0.05	83.59%±0.85%	84.81%±2.71%	84.16%±7.16%
	AC [8] w/o	0.13	3.09	0.81	0.55	1.05	83.68%±1.43%	81.89%±2.43%	88.48%±1.96%
	ADG [4] w/o	0.13	3.02	0.79	0.10	0.87	85.72%±2.25%	80.95%±3.10%	86.07%±2.87%
	METEOR [5] w/o	0.12	2.97	0.79	0.29	0.84	85.52%±1.42%	79.66%±0.73%	81.71%±5.49%
	DISCOP [6] w/o	0.12	3.00	0.80	0.25	3.41	83.61%±3.21%	81.44%±4.00%	84.31%±2.84%
	RS w/	0.30	3.07	0.81	/	4.37	69.67%±1.98%	64.81%±2.71%	70.27%±3.12%
	AC [8] w/	0.34	3.20	0.82	0.56	3.66	74.23%±1.21%	67.23%±4.00%	71.23%±5.65%
	ADG [4] w/	0.30	2.85	0.79	0.12	5.67	72.65%±3.64%	65.45%±1.87%	67.51%±3.86%
	METEOR [5] w/	0.31	3.05	0.81	0.32	7.65	71.34%±4.21%	64.16%±3.61%	68.91%±2.34%
	DISCOP[6] w/	0.30	3.00	0.82	0.28	6.60	65.23%±1.85%	68.68%±2.95%	70.39%±2.21%
LLAMA3 [15]	RS w/o	0.12	3.79	0.80	/	0.65	88.10%±3.35%	81.80%±4.50%	90.80%±4.03%
	AC [8] w/o	0.12	3.96	0.82	0.64	0.48	88.62%±2.62%	84.92%±1.70%	87.07%±3.90%
	ADG [4] w/o	0.12	3.76	0.80	0.19	0.60	89.29%±3.33%	83.80%±4.50%	87.88%±1.96%
	METEOR [5] w/o	0.13	3.79	0.81	0.36	0.73	91.31%±1.53%	81.41%±2.58%	90.40%±2.25%
	DISCOP [6] w/o	0.12	3.88	0.80	0.31	0.66	88.07%±2.64%	82.33%±3.05%	87.80%±6.54%
	RS w/	0.34	3.78	0.81	/	5.00	69.53%±3.42%	67.80%±4.50%	78.21%±2.45%
	AC [8] w/	0.36	4.03	0.84	0.69	6.54	68.25%±3.12%	69.23%±3.56%	79.22%±3.91%
	ADG [4] w/	0.39	3.78	0.83	0.22	5.00	72.13%±1.94%	69.35%±3.87%	77.33%±3.62%
	METEOR [5] w/	0.41	4.13	0.84	0.41	8.25	66.49%±2.13%	68.31%±1.43%	70.92%±1.49%
	DISCOP [6] w/	0.39	3.88	0.80	0.34	8.35	67.14%±3.94%	68.53%±1.82%	71.23%±1.72%
MISTRAL v0.3 [13]	RS w/o	0.19	4.03	0.90	/	0.59	86.43%±5.32%	80.07%±5.13%	89.56%±3.51%
	AC [8] w/o	0.18	3.91	0.88	0.95	0.55	87.03%±2.02%	81.06%±1.12%	90.52%±3.26%
	ADG [4] w/o	0.19	4.16	0.93	0.44	1.12	86.95%±1.78%	88.91%±3.27%	92.43%±3.15%
	METEOR [5] w/o	0.19	4.01	0.90	0.60	0.54	87.15%±2.14%	83.88%±3.99%	91.07%±3.68%
	DISCOP [6] w/o	0.19	4.03	0.91	0.49	0.56	86.95%±2.57%	85.77%±1.45%	85.42%±4.31%
	RS w/	0.44	3.96	0.89	/	3.00	75.82%±1.32%	66.66%±0.73%	76.23%±3.59%
	AC [8] w/	0.41	3.75	0.88	0.97	5.26	72.03%±1.66%	68.46%±5.42%	76.90%±1.08%
	ADG [4] w/	0.44	4.34	0.94	0.48	4.17	74.39%±3.45%	70.06%±1.12%	79.55%±1.13%
	METEOR [5] w/	0.48	4.29	0.92	0.70	4.22	74.13%±2.89%	68.95%±1.28%	74.46%±3.59%
	DISCOP [6] w/	0.44	4.17	0.91	0.50	2.91	75.46%±1.38%	66.67%±1.98%	70.89%±2.26%
QWEN2 [12]	RS w/o	0.12	2.35	0.73	/	0.53	85.88%±1.13%	81.75%±3.23%	84.61%±3.68%
	AC [8] w/o	0.13	2.53	0.74	0.65	0.66	85.36%±3.39%	84.74%±2.45%	80.92%±4.26%
	ADG [4] w/o	0.13	2.39	0.74	0.20	0.69	85.90%±2.94%	88.07%±2.12%	87.39%±1.10%
	METEOR [5] w/o	0.13	2.36	0.73	0.36	0.57	85.05%±4.64%	80.61%±2.85%	83.91%±5.77%
	DISCOP [6] w/o	0.13	2.34	0.73	0.31	0.53	85.36 %±4.32%	83.01%±3.01%	83.08%±4.59%
	RS w/	0.38	2.45	0.75	/	2.79	71.38%±1.29%	70.78%±2.12%	63.30%±3.49%
	AC [8] w/	0.37	2.45	0.75	0.70	1.90	72.82%±1.07%	72.61%±0.88%	67.67%±2.82%
	ADG [4] w/	0.37	2.39	0.75	0.23	2.60	71.38%±1.09%	71.27%±1.56%	72.13%±3.98%
	METEOR [5] w/	0.38	2.43	0.74	0.41	2.38	71.12%±3.38%	60.56%±2.19%	65.92%±1.18%
	DISCOP [6] w/	0.33	2.42	0.76	0.32	1.76	72.13%±1.12%	70.27%±1.28%	69.28%±3.19%

TABLE II
XHS MAIN RESULT. "W/O" INDICATES MODELS WITHOUT FREStEGA, WHILE "W/" INDICATES MODELS WITH FREStEGA.

Model	Algorithm	Linguistics		Capacity		Domain Statistical Imperceptibility			
		Div.↑	PPL↓	Entro./token↑	ER ↑	MAU. (%)↑	CSW-F1↓	RNN-F1↓	r-bilstm-c-F1↓
QWEN2[12]	RS w/o	0.74	15.83	2.22	/	73.18	89.08%±2.64%	85.18%±0.98%	79.73%±2.64%
	AC[8] w/o	0.76	11.08	2.08	2.83	70.14	90.41%±2.62%	79.94%±3.26%	80.24%±1.48%
	ADG[4] w/o	0.76	21.35	2.06	1.93	63.54	94.94%±1.16%	74.19%±3.60%	83.34%±2.10%
	METEOR[5] w/o	0.73	16.19	2.18	1.48	73.69	89.15%±1.29%	80.26%±1.95%	85.82%±2.93%
	DISCOP[6] w/o	0.78	11.02	2.13	1.13	74.63	87.81%±2.15%	86.53%±4.56%	87.22%±3.77%
	RS w/	0.80	15.77	2.30	/	91.05	57.79%±1.81%	47.05%±2.63%	66.43%±2.94%
	AC[8] w/	0.78	11.11	2.17	2.99	93.97	52.85%±3.24%	50.05%±2.74%	71.28%±1.38%
	ADG[4] w/	0.79	19.17	2.31	2.43	91.72	60.79%±1.41%	52.77%±1.65%	73.31%±3.36%
	METEOR[5] w/	0.78	12.35	2.18	2.15	93.20	53.61%±2.71%	47.05%±2.74%	69.21%±1.43%
	DISCOP[6] w/	0.81	13.61	2.17	1.16	92.47	55.56%±2.90%	45.77%±2.55%	65.29%±1.16%
CHATGLM3[52]	RS w/o	0.75	319.62	4.55	/	26.44	62.19%±4.50%	68.23%±4.99%	76.01%±1.17%
	AC[8] w/o	0.75	308.82	4.56	4.23	27.87	68.51%±3.37%	77.55%±3.04%	74.44%±3.43%
	ADG[4] w/o	0.77	394.76	4.61	4.36	54.43	79.95%±0.79%	72.73%±1.42%	78.43%±1.30%
	METEOR[5] w/o	0.70	284.99	4.08	2.27	31.35	69.02%±3.81%	73.82%±4.56%	64.52%±3.11%
	DISCOP[6] w/o	0.75	311.86	4.52	1.29	27.78	65.80%±4.59%	74.62%±3.77%	75.44%±3.43%
	RS w/	0.78	366.74	4.67	/	80.17	44.44%±1.43%	43.44%±3.21%	34.23%±2.92%
	AC[8] w/	0.77	366.31	4.66	4.53	93.21	47.21%±1.51%	45.77%±2.99%	38.59%±2.31%
	ADG[4] w/	0.79	394.53	4.88	4.82	71.11	52.33%±1.02%	52.26%±1.42%	54.78%±1.29%
	METEOR[5] w/	0.78	365.81	4.66	3.44	90.61	44.16%±3.26%	43.85%±1.01%	41.26%±2.35%
	DISCOP[6] w/	0.77	363.70	4.62	1.39	90.02	45.77%±2.55%	44.15%±2.33%	43.58%±2.39%

TABLE III
SHAKESPEARE MAIN RESULT. "W/O" INDICATES MODELS WITHOUT FRESTEGA, WHILE "W/" INDICATES MODELS WITH FRESTEGA.

Model	Algorithm	Linguistics		Capacity		Domain Statistical Imperceptibility			
		Div.↑	PPL↓	Entro./token↑	ER ↑	MAU. (%)↑	CSW-F1↓	RNN-F1↓	r-bilstm-c-F1↓
LLAMA2[14]	RS w/o	0.30	4.17	0.83	/	9.12	93.39%±1.02%	94.81%±0.93%	96.52%±0.50%
	AC[8] w/o	0.30	4.13	0.83	0.32	9.09	94.29%±1.05%	95.21%±0.92%	96.31%±0.32%
	ADG[4] w/o	0.29	4.09	0.80	8.76	0.27	94.45%±0.25%	96.93%±0.77%	96.53%±0.63%
	METEOR[5] w/o	0.29	4.10	0.80	0.28	9.32	93.25%±1.20%	96.22%±0.87%	96.00%±0.73%
	DISCOP[6] w/o	0.29	4.09	0.81	0.14	8.08	95.25%±1.40%	97.16%±0.07%	96.99%±0.48%
	RS w/	0.44	4.38	0.83	/	19.52	69.96%±2.26%	70.13%±2.27%	70.81%±7.49%
	AC[8] w/	0.43	4.58	0.85	0.38	20.15	69.56%±1.12%	69.98%±1.37%	72.17%±4.56%
	ADG[4] w/	0.44	4.42	0.83	0.35	22.47	67.01%±1.82%	66.62%±2.90%	68.45%±2.59%
	METEOR[5] w/	0.44	4.32	0.84	21.99	0.21	68.96%±1.12%	68.80%±1.83%	70.89%±5.60%
	DISCOP[6] w/	0.43	4.29	0.83	0.17	24.64	67.52%±1.81%	66.62%±2.90%	70.46%±3.12%
LLAMA3[15]	RS w/o	0.35	3.86	0.70	/	0.54	83.70%±0.48%	87.64%±1.34%	86.00%±0.29%
	AC[8] w/o	0.36	3.83	0.70	0.36	0.54	84.92%±0.32%	89.14%±2.46%	87.39%±1.69%
	ADG[4] w/o	0.36	3.84	0.71	0.33	0.49	81.02%±4.88%	86.35%±1.51%	85.47%±1.95%
	METEOR[5] w/o	0.36	3.84	0.71	0.23	0.56	82.27%±2.12%	87.23%±0.49%	84.78%±1.40%
	DISCOP[6] w/o	0.36	3.83	0.71	0.17	0.56	83.13%±0.78%	86.95%±0.59%	85.21%±0.99%
	RS w/	0.47	3.82	0.70	/	2.08	60.91%±2.25%	58.62%±3.92%	62.03%±3.80%
	AC[8] w/	0.48	3.93	0.71	0.39	2.03	61.27%±1.32%	59.74%±1.69%	65.09%±3.35%
	ADG[4] w/	0.49	3.94	0.73	0.37	3.14	61.29%±1.07%	57.41%±1.31%	64.33%±2.08%
	METEOR[5] w/	0.49	3.96	0.71	0.26	1.95	59.56%±4.52%	54.72%±1.67%	65.48%±3.70%
	DISCOP[6] w/	0.49	3.99	0.71	0.18	2.60	58.87%±3.08%	57.41%±4.31%	65.71%±2.58%
MISTRAL V0.3[13]	RS w/o	0.34	4.07	0.72	/	1.04	84.86%±0.82%	88.37%±0.71%	85.60%±1.18%
	AC[8] w/o	0.37	4.07	0.72	0.23	1.18	86.31%±1.95%	90.36%±2.47%	86.73%±2.04%
	ADG[4] w/o	0.37	4.07	0.71	0.22	1.14	83.17%±0.80%	88.55%±0.57%	86.95%±1.45%
	METEOR[5] w/o	0.37	4.06	0.72	0.16	0.74	83.55%±1.45%	88.04%±0.86%	86.86%±0.34%
	DISCOP[6] w/o	0.37	4.05	0.72	0.11	1.29	83.59%±1.29%	87.58%±0.64%	86.52%±0.30%
	RS w/	0.49	4.02	0.73	/	35.75	59.67%±2.78%	65.57%±1.87%	66.21%±3.60%
	AC[8] w/	0.49	4.11	0.73	0.26	29.73	59.32%±3.02%	64.82%±2.30%	66.27%±3.29%
	ADG[4] w/	0.49	4.00	0.72	0.24	12.10	59.22%±3.58%	63.27%±4.86%	67.24%±2.43%
	METEOR[5] w/	0.48	4.18	0.74	0.17	23.45	57.13%±1.75%	64.84%±2.30%	66.30%±4.14%
	DISCOP[6] w/	0.49	4.25	0.73	0.12	37.56	58.32%±1.86%	63.96%±2.27%	66.32%±3.16%
QWEN2[12]	RS w/o	0.39	3.06	0.72	/	0.98	82.10%±1.15%	81.17%±0.36%	81.06%±1.76%
	AC[8] w/o	0.40	3.06	0.72	0.46	0.50	83.97%±2.71%	82.88%±2.06%	82.15%±1.56%
	ADG[4] w/o	0.40	3.06	0.73	0.43	2.18	81.93%±0.74%	81.38%±1.02%	80.36%±0.92%
	METEOR[5] w/o	0.40	3.07	0.73	0.31	4.27	80.68%±1.45%	68.61%±2.85%	80.26%±1.28%
	DISCOP[6] w/o	0.40	3.07	0.73	0.20	0.96	80.84%±1.00%	81.17%±2.01%	81.54%±1.20%
	RS w/	0.51	3.04	0.74	/	9.04	58.46%±2.87%	52.63%±1.68%	62.36%±3.83%
	AC[8] w/	0.51	3.19	0.76	0.49	8.80	57.18%±2.58%	52.21%±4.68%	62.34%±3.92%
	ADG[4] w/	0.51	3.03	0.75	0.44	14.21	54.92%±2.21%	54.41%±4.67%	64.26%±3.73%
	METEOR[5] w/	0.51	3.20	0.74	0.33	14.29	55.58%±2.86%	53.98%±3.14%	61.38%±3.65%
	DISCOP[6] w/	0.52	3.18	0.75	0.21	8.19	58.60%±2.77%	52.63%±3.63%	62.40%±3.57%

C. Performance Evaluation

The experimental results of FreStega on the IMDB, XHS, and Shakespeare datasets are shown in Table I, Table II and Table III, respectively. Note that the term "RS" refers to random sampling in language models without embedding any hidden messages, representing the ideal secure steganography. In the main experiment, we set $c = 0.1$ and $\alpha = 0.1$. From these results, we have the following findings.

1) *Imperceptibility*: Even with advanced distribution-preserving methods like METEOR [5] or DISCOP [6], stego-texts remain easily distinguishable from the cover text in real-world scenarios, as reflected by both MAUVE and steganalysis F1. FreStega significantly improves imperceptibility across most scenarios, as evidenced by increased MAUVE scores and decreased detector F1. It better aligns stego text distribution with human text in the target domain. We analyzed the word frequencies of stego texts generated using the baseline and FreStega. We observed that our method introduced some words that had not appeared before, which have a distinct style characteristic of the target corpus. For example, words like 'tempest', 'alas' and other Shakespearean-style words appear

after our alignment. In the case of the XHS platform, the language model has learned to emulate its corresponding flamboyant style. Emojis appear more in aligned XHS stego text. These nuanced linguistic features, beyond simple semantic attributes, highlight the complexity of human language. FreStega refines the language model's distribution, making stego texts more aligned with the target domain and harder to detect.

To further simulate the content detection faced by stego-texts on real-world internet platforms, we conducted experiments using Fast-DetectGPT [56], currently the state-of-the-art method in AIGT detection, with its default multilingual setting (using davinci-002 as the scoring model). The results are presented in Table IV. The results consistently demonstrate that, by aligning with texts in the target domain, FreStega enhances the imperceptibility of stego texts from the perspective of AIGT classifiers.

2) *Linguistic Quality*: In terms of linguistic quality, it is evident that the diversity of stego texts generated by baseline methods is significantly lower than that of human text, particularly in the IMDB and SHAKESPEARE datasets, as reflected

TABLE IV
FAST-DETECTGPT DETECTION RESULTS. EACH ENTRY IN THE TABLE REPRESENTS THE AVERAGE PROBABILITY THAT FAST-DETECTGPT CLASSIFIES THE STEGOTEXT AS AI-GENERATED (AI PROB).

Dataset	SHAKESPERE					IMDB					XHS				
	RS	AC	ADG	Met.	Dis.	RS	AC	ADG	Met.	Dis.	RS	AC	ADG	Met.	Dis.
LLAMA2 w/o	0.45	0.45	0.47	0.43	0.47	0.85	0.84	0.85	0.85	0.86	-	-	-	-	-
LLAMA2 w/	0.42	0.41	0.39	0.41	0.40	0.82	0.81	0.83	0.82	0.79	-	-	-	-	-
LLAMA3 w/o	0.41	0.40	0.42	0.40	0.41	0.75	0.70	0.74	0.75	0.85	-	-	-	-	-
LLAMA3 w/	0.37	0.36	0.36	0.36	0.37	0.71	0.69	0.68	0.71	0.74	-	-	-	-	-
MISTRAL w/o	0.36	0.36	0.38	0.36	0.36	0.52	0.56	0.50	0.53	0.53	-	-	-	-	-
MISTRAL w/	0.33	0.34	0.33	0.35	0.34	0.50	0.53	0.47	0.50	0.47	-	-	-	-	-
QWEN2 w/o	0.40	0.38	0.39	0.38	0.38	0.68	0.71	0.65	0.69	0.71	0.43	0.42	0.46	0.40	0.39
QWEN2 w/	0.34	0.34	0.34	0.35	0.35	0.63	0.66	0.63	0.63	0.65	0.37	0.39	0.42	0.37	0.38
CHATGLM3 w/o	-	-	-	-	-	-	-	-	-	-	0.75	0.75	0.76	0.78	0.79
CHATGLM3 w	-	-	-	-	-	-	-	-	-	-	0.70	0.69	0.70	0.68	0.69

by the *distinct3*. A major reason existing baseline methods are easily detected is that their language model distribution is too sharp, causing the generated stego text to fall into a few fixed patterns. In contrast, FreStega adjusts the language model distribution to alleviate the sharpening phenomenon, effectively increasing the diversity of stego text in almost all scenarios. Similarly, our method ensures the fluency of the generated text, with the perplexity being almost identical to that of baseline methods. In most cases, since FreStega mitigates the distribution sharpness issue in language models, incorporating FreStega leads to a slight increase in perplexity, typically by no more than 5%—except for ChatGLM3-6B. In a few cases, PPL may even decrease, but overall it remains roughly comparable to the baseline without FreStega. Although PPL is not a perfect metric, our experiment results indicate that FreStega does not introduce overly strong control signals during the target domain alignment process, which would force the language model to produce nonsensical text or fall into the other extreme of obvious repetition. In a word, FreStega effectively preserves the meaningfulness and coherence of the stego text, even as it enhances the entropy in the sequential alignment stage.

3) *Capacity*: In terms of capacity, FreStega consistently and reliably increases the embedding rate across all scenarios. FreStega achieved a relative increase in embedding rates of 20.65%, 10.07%, and 15.94% on the XHS, IMDB, and SHAKESPEARE datasets, respectively. This aligns with FreStega’s intended goal of using temporal alignment to raise the entropy of the language model’s distribution while maintaining text quality, thereby increasing the upper limit of capacity compared to the original. Experiments confirm that FreStega effectively increases the embedding rate while preserving text quality.

D. Time Efficiency

1) *Preprocessing Time Efficiency Analysis*: Before performing alignment in the spatial dimension, FreStega requires preprocessing to calculate the token frequency of the dataset. This preprocessing mainly focuses on handling the target-

domain corpus, as naturally generated model data is relatively easier to obtain in advance. To demonstrate FreStega’s efficiency, we measured preprocessing time across datasets of varying types and sizes. In our case, preprocessing only involves token counting with a language model tokenizer on CPUs, requiring minimal resources and running at high speed. The preprocessing requires minimal resources and operates at a very high speed. We report the average results from three repeated trials using the QWEN2 tokenizer (VocabSize is 151643) on $24 \times$ Intel Xeon w5-3423 CPUs, as shown in Table VI. As the results indicate, FreStega introduces no significant time overhead during the preprocessing stage. Additionally, preprocessing is performed only once; subsequent inferences require no reprocessing. Figure 5 shows the average amortized time per inference as the number of inferences increases, based on preprocessing 1 million tokens and generating 200 tokens per run. The amortized time over n runs is defined as:

$$T_{\text{amortized}}^{(n)} = \frac{\sum_{i=1}^n T_{\text{inference}}^{(i)} + T_{\text{preprocess}}}{n}, \quad (22)$$

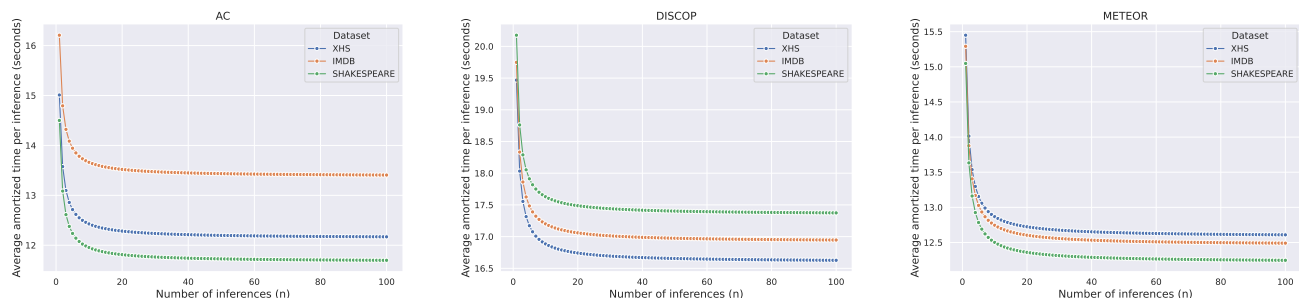
where $T_{\text{inference}}^{(i)}$ denotes the time taken for the i -th inference, and $T_{\text{preprocess}}$ represents the fixed cost of preprocessing. As shown in Figure 5, as the number of inferences increases, the effective amortized cost of preprocessing becomes negligible, and the amortized time per inference quickly converges to the time required to generate a single sentence (200 tokens).

When the target domain dataset is updated, FreStega is adaptive and does not require reprocessing the entire dataset. Instead, when new data points are introduced in the target application domain, FreStega only needs to compute the token frequencies for the new data—a simple tokenizer-based count without any need for model inference. The updated frequency statistics are linearly merged with the existing table. We evaluated time and memory overhead under such dataset updates. As shown in Table VII, FreStega incurs no significant overhead in dynamic update scenarios.

2) *Generation Time Efficiency Analysis*: The time efficiency of steganography schemes depends on both the language model’s generation speed and the steganography algo-

TABLE V
AVERAGE TIME EFFICIENCY (MS/TOKEN) FOR 1000 SAMPLES TESTED ON DIFFERENT MODELS ACROSS SHAKESPEARE, IMDB, AND XHS.

Dataset	SHAKESPERE					IMDB					XHS					p-value
	RS	AC[8]	ADG[4]	Met.[5]	Dis.[6]	RS	AC[8]	ADG[4]	Met.[5]	Dis.[6]	RS	AC[8]	ADG[4]	Met.[5]	Dis.[6]	
LLAMA2[14] w/o	52.19	52.15	61.13	52.43	56.72	58.54	56.19	59.79	54.66	60.62	-	-	-	-	-	0.8640
LLAMA2[14] w/	52.07	53.19	62.27	53.69	57.12	56.75	55.85	58.26	55.72	60.12	-	-	-	-	-	
LLAMA3[15] w/o	63.17	61.19	102.99	61.59	81.44	71.09	72.47	76.61	62.74	81.56	-	-	-	-	-	0.5537
LLAMA3[15] w/	68.05	61.67	108.02	64.58	88.42	63.74	63.86	76.87	68.25	81.74	-	-	-	-	-	
MISTRAL v0.3[13] w/o	56.74	56.72	66.31	56.93	65.29	58.13	57.79	63.45	58.74	63.69	-	-	-	-	-	0.1351
MISTRAL v0.3[13] w/	57.85	56.64	66.13	58.12	66.27	58.43	63.14	63.41	59.06	63.40	-	-	-	-	-	
QWEN2[12] w/o	58.49	57.74	106.05	57.76	81.21	68.55	66.01	75.94	60.47	84.67	58.72	58.68	150.28	58.75	81.55	0.3603
QWEN2[12] w/	62.27	58.35	109.24	61.09	86.73	74.67	66.89	76.81	62.31	84.59	60.84	60.70	120.23	62.90	82.99	
CHATGLM3[52] w/o	-	-	-	-	-	-	-	-	-	-	29.42	29.76	46.76	30.71	38.87	0.1199
CHATGLM3[52] w	-	-	-	-	-	-	-	-	-	-	30.17	30.40	46.98	30.43	39.35	



(a) Average amortized time per inference for the AC algorithm (b) Average amortized time per inference for the METEOR algorithm (c) Average amortized time per inference for the DISCOP algorithm

Fig. 5. Average Amortized Time per Inference using QWEN2

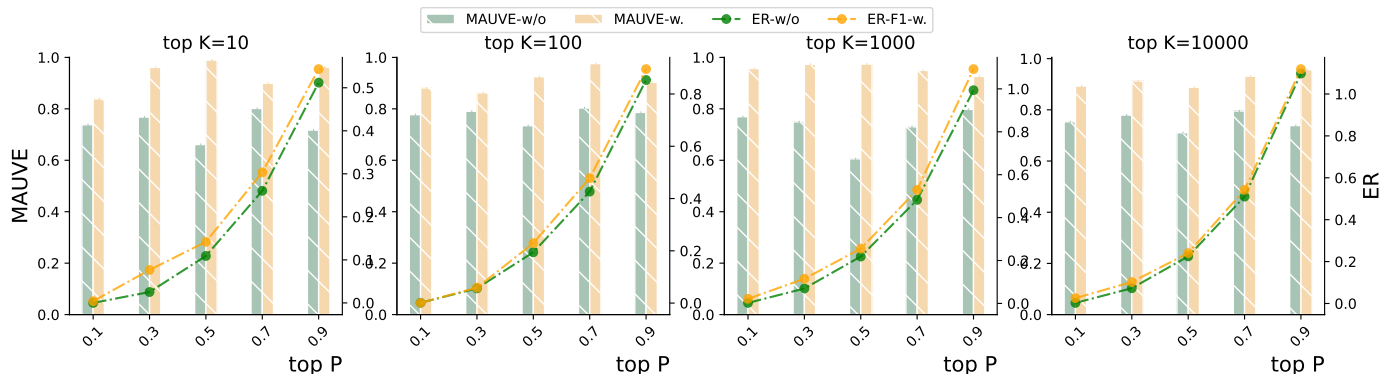


Fig. 6. Top-p and Top-k performance on MAUVE and Embedding Rate (ER) using Qwen-DISCOP

TABLE VI
PREPROCESSING TIME FOR DIFFERENT DATASETS

Dataset	Number of Entries	Token Count	Total Processing Time (s)	Average Processing Time/Token (s)
XHS [4]	1,508	588,334	1.69	2.87×10^{-6}
IMDB [5]	1,039,403	25,809,893	73.04	2.83×10^{-6}
SHAKESPERE [6]	18,395	241,212	1.04	4.32×10^{-6}
TWEET [7]	2,588,579	24,030,017	140.18	5.83×10^{-6}
AG-NEWS [8]	2,000	101,624	0.51	4.97×10^{-6}
WILD [9]	4,000	630,467	2.13	3.38×10^{-6}
SST2 [10]	67,348	821,928	4.51	5.49×10^{-6}
PubMedQA [11]	50,000	2,688,268	9.58	3.57×10^{-6}
MBA_BAIKE [12]	10,688	13,504,157	33.54	2.48×10^{-6}
CHINESE-MEDICAL [13]	792,099	84,744,361	161.11	1.90×10^{-6}

rithm’s time complexity. As shown in Table V, incorporating FreStega does not negatively impact token generation time. In fact, the generation speed remains almost unchanged, and in some cases, is even faster. We conducted *paired t-tests* to com-

pare the time taken with and without FreStega for each model. As shown in the far-right column of the table V, the *p-values* for all models are greater than 0.05, indicating that FreStega does not introduce a statistically significant difference in time efficiency. As for the steganographic algorithm, ADG incurs higher time costs due to its dynamic grouping, while METEOR operates without reordering, keeping time costs lower. This also demonstrates the efficiency of FreStega as a plug-and-play module, as it does not introduce any additional computational overhead to the covert communication system.

E. Compatibility analysis

1) *Compatibility with prompt-based methods and fine-tuning methods:* Since the FreStega method operates at the language model’s decoding stage, it is compatible with

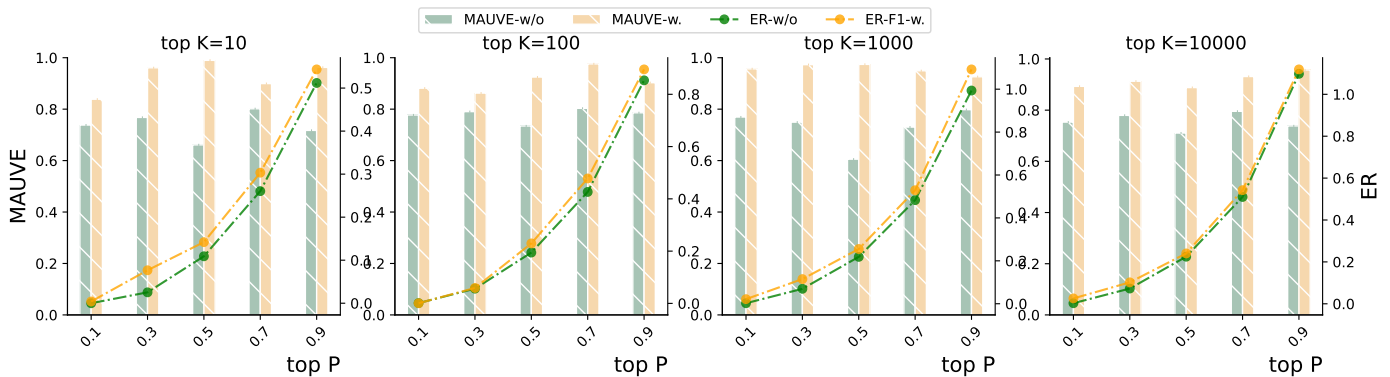


Fig. 7. Top-p and Top-k performance on MAUVE and Embedding Rate (ER) using Qwen-METEOR

TABLE VII
PREPROCESSING TIME AND MEMORY USAGE REQUIRED DURING TARGET DOMAIN DATASET UPDATES

Dataset	New data points	New Tokens	Total Processing Time (ms)	Memory Overhead (MB)
XHS	25	7634	0.1090	869.3711
	50	20096	0.1392	873.8711
	100	39062	0.1736	870.1523
	300	113967	0.2991	878.2422
	500	196970	0.4786	875.2422
	700	269522	0.6514	880.5195
	900	349602	0.7511	878.1406
	1000	388885	0.8038	881.6562
IMDB	1300	504994	1.0673	881.5664
	1500	585138	1.2063	884.1719
	100	2406	0.0977	1038.6562
	500	13088	0.1388	1045.2305
	1000	26117	0.1752	1039.2227
	2000	51993	0.2541	1044.4453
Shakespeare	3000	78175	0.3304	1041.4219
	4000	103537	0.4332	1045.6328
	5000	128851	0.4949	1043.3672
	100	1263	0.0937	969.0234
	500	6809	0.1127	968.7734
	1000	12719	0.1345	921.7545
Shakespeare	2000	26535	0.2298	914.3140
	3000	38872	0.2468	911.3164
	4000	51481	0.2741	910.8164
	5000	65505	0.4587	908.0664

both prompt-based and fine-tuning-based approaches. For the prompt-guided approach, we designed zero-shot prompts tailored to the XHS domain and few-shot prompts following the design in ZGLS [57]. The prompts used in the zero-shot setting and few-shot setting are shown in the Appendix VI-B.

For the fine-tuned approach, we employed LoRA to fine-tune QWEN2-7B on target domain data, with detailed fine-tuning parameters provided in Table XI in the Appendix VI-B. The compatibility experiment results (Table VIII) show that prompt-based methods still require carefully crafted prompts, while fine-tuning methods demand substantial computational resources and require retraining when faced with new target domains. In contrast, FreStega operates purely at the decoding stage, offering a lightweight, plug-and-play enhancement that integrates seamlessly with fine-tuning or prompt-based methods, effectively improving the practical imperceptibility and embedding capacity of the generated stegotext.

2) *Compatibility with sampling strategy*: Since the core of the FreStega method lies in distribution adjustment without imposing any constraints on the sampling strategies applied over

Method	Setting	Algorithm	MAUVE \uparrow	TS-CSW FI [3] \downarrow	ER \uparrow
Prompt-based	Zero-shot	METEOR	81.94%	71.72% \pm 2.87%	2.05
		DISCOP	80.41%	71.98% \pm 2.93%	1.15
		METEOR+ours	89.25%	59.40% \pm 3.74%	2.10
	Few-shot[57]	DISCOP+ours	88.42%	60.12% \pm 3.81%	1.16
		METEOR	83.32%	70.83% \pm 1.83%	1.81
		DISCOP	85.59%	68.84% \pm 2.07%	1.16
Fine-tuning-based	LoRA	METEOR+ours	94.89%	53.77% \pm 2.46%	1.85
		DISCOP+ours	93.14%	54.97% \pm 1.83%	1.23
		METEOR	95.27%	53.14% \pm 3.03%	2.63
	LoRA	DISCOP	92.31%	54.07% \pm 3.16%	1.86
		METEOR+ours	95.92%	50.05% \pm 2.31%	2.68
		DISCOP+ours	93.99%	52.64% \pm 3.18%	1.93

TABLE VIII
COMPATIBILITY EXPERIMENTS BETWEEN FRESTEGA AND FINE-TUNING-BASED METHODS AS WELL AS PROMPT-BASED METHODS

the adjusted distribution, FreStega is inherently compatible with various sampling methods. In this section, we primarily analyze the compatibility of FreStega with top- p and top- k sampling strategies. In main experiments, we used tokens from the full vocabulary for steganographic sampling without restricting the vocabulary size (top- $p=1$, top- $k=VocabSize$). The main results in Tab. I, II, III demonstrate that FreStega effectively mitigates the phenomenon of distribution sharpening and achieves better alignment with the target domain distribution. We evaluate the DISCOP and METEOR methods on the QWEN2 XHS dataset under various top- p and top- k settings, following the default order of first applying top- k truncation, followed by top- p filtering. As shown in Figure 6 and Figure 7, FreStega remains effective under various conditions and is compatible with these sampling strategies. In terms of embedding capacity, the experimental results show that constraining top- p or top- k sampling does not provide benefit for embedding capacity. Therefore, we adopt by default a strategy that uses the full vocabulary without truncation.

F. Applicability to LLMs of different sizes

FreStega is adaptable across various models scales. In our main experiments, we primarily employed 7B-sized models. To further evaluate its effectiveness and generalizability, we tested FreStega on the QWEN2 series spanning a range of model sizes. Specifically, we assessed full-precision models with 1.5B, 7B, 14B, and 32B parameters using zero-shot prompts on the XHS dataset, measuring MAUVE scores and

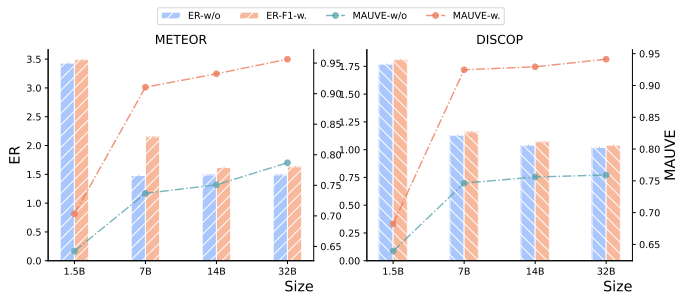


Fig. 8. Results of stegotexts generated by QWEN2 of different sizes

embedding rates (ER) over 1,000 generated samples. As shown in Figure 8, FreStega exhibits strong generalization, working effectively across language models of different sizes while enhancing both imperceptibility and embedding capacity. Notably, the ER drops significantly when transitioning from 1.5B to 7B models, reflecting the tendency of larger models to generate more deterministic outputs—a phenomenon known as distribution sharpening—which, as previously discussed, presents a practical challenge by potentially reducing steganographic capacity.

G. Control Intensity of Alignment

For FreStega, we explored two key hyperparameters—spatial alignment intensity α and sequential alignment intensity c —using DISCOP on QWEN2 as the representative steganography scheme with a base temperature of 1.

As Figure 9 shows, increasing α leads to better alignment with the target human text distribution, reflected in higher MAUVE values, while maintaining statistical imperceptibility. Although higher α enhances imperceptibility, the benefits stabilize, making extensive tuning unnecessary; Empirically, $\alpha = 0.1$ generally works well. The sequential alignment intensity c slightly adjusts the temperature based on the distribution’s entropy, offering a global adjustment. While higher temperatures can increase text diversity, they may also add unnecessary noise. As shown in Figure 10, we empirically set $c = 0.1$ to improve embedding capacity while maintaining imperceptibility. While not optimal, these hyperparameters perform well in most cases without further tuning.

Further, practically speaking, automatic hyperparameter optimization methods such as grid search can be employed. Specifically, we first generate small batches of stegotext using FreStega on a small dataset (e.g., 500 samples) and then perform grid search over the hyperparameters α and c on this subset to identify optimal configurations. The grid search results are presented in Figure 11. FreStega achieves robust alignment with the target domain across a broad range of hyperparameter values (with MAUVE scores exceeding 0.8 in most cases). Although our default settings ($c = 0.1$, $\alpha = 0.1$) do not yield the absolute highest MAUVE scores, they consistently deliver strong performance across nearly all conditions. Moreover, since hyperparameter tuning is a black-box optimization problem, users can efficiently apply methods like Random Search [58] or Bayesian Optimization [59] to find optimal settings.

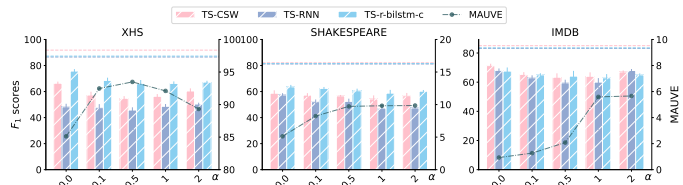


Fig. 9. Hyperparameter analysis of α ($c=0.1$). We tested the F1 scores of classifiers on three datasets (XHS, SHAKESPEARE, IMDB) using three classic steganalysis methods (TS-CSW [17], TS-RNN [18], TS-r-bilstm-c [19]). The corresponding colored lines indicate the F1 scores of the steganalysis methods without FreStega. The green dashed line represents the MAUVE score relative to the target domain text.

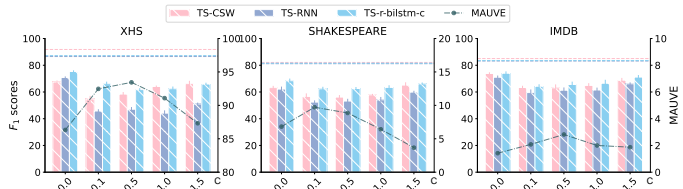


Fig. 10. Hyperparameter analysis of c ($\alpha=0.1$). We tested the F1 scores of classifiers on three datasets (XHS, SHAKESPEARE, IMDB) using three classic steganalysis methods (TS-CSW [17], TS-RNN [18], TS-r-bilstm-c [19]). The corresponding colored horizontal lines indicate the F1 scores of the steganalysis methods without FreStega. The green dashed line represents the MAUVE score relative to the target domain text.

H. Quantity of Target Domain Texts Used for Alignment

In the main experiment, we used the entire target domain text we can obtain for alignment. In subsequent analyses, we discuss in detail the impact of the amount of target domain data required for effective alignment. We experimented with different quantities of target domain text for alignment on the XHS dataset using two models, QWEN2 and CHATGLM, to assess the impact on stego text generation. The XHS dataset contains a total of 1,508 texts. To eliminate model bias, we fixed the model to generate 2,000 texts. We then used 25, 50, 100, 300, 500, 700, 1,000, 1,300, and 1,500 target domain texts for spatial alignment. The results are shown in Figure 12 and Figure 13. From the figures, we can see that more alignment samples lead to better domain imperceptibility and higher fluency. However, it is unnecessary to capture an excessive amount of target domain text for distribution alignment. The experimental results suggest two reasons for this: First, FreStega requires only a small amount of target domain text—around 100 samples—to effectively exhibit the characteristics of the target domain and closely match its distribution. This means that even if target-aligned domain data is difficult to obtain, FreStega requires only a small number of samples for alignment, enabling rapid adaptation to the environment. Second, an interesting phenomenon occurs when the number of alignment samples exceeds a certain threshold; the gains from distribution alignment gradually slow down and stabilize. This indicates a diminishing marginal return in imperceptibility gains as the amount of target domain text increases.

Even without access to any target domain data, the Sequential Adjustment of FreStega remains effective, successfully alleviating the inherent sharpening tendencies of the language

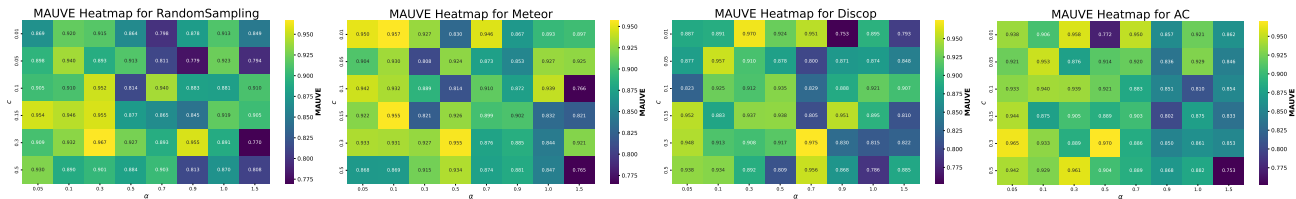


Fig. 11. Heatmaps showing MAUVE scores under different (α, c) settings for RandomSampling, METEOR, DISCOP, and AC on XHS.

model, which is particularly effective when the target corpus, such as XHS, exhibits high diversity.

V. CONCLUSION

We propose a plug-and-play probability distribution reconstruction method to enhance the imperceptibility and embedding capacity of generative linguistic steganography in real-world scenarios. State-of-the-art distribution-preserving steganography methods are closely tied to the language model’s native distribution, leading to a mismatch with real-world cover texts. To address the resulting imperceptibility gap, we reconstruct the model distribution to align with the target domain across both sequential and spatial dimensions, enabling a more suitable and realistic channel for steganographic sampling. FreStega seamlessly integrates with existing generative steganography algorithms and various language models. Stego texts generated by FreStega demonstrate higher embedding capacity while maintaining linguistic quality, exhibiting strong imperceptibility against various steganalysis detectors in real-world scenarios.

REFERENCES

- [1] P. Syverson, R. Dingleline, and N. Mathewson, “Tor: The secondgeneration onion router,” in *Usenix Security*. USENIX Association Berkeley, CA, 2004, pp. 303–320.
- [2] Z. Yang, K. Chen, K. Zeng, W. Zhang, and N. Yu, “Provably secure robust image steganography,” *IEEE Transactions on Multimedia*, 2023.
- [3] K. Gopalan, “Audio steganography using bit modification,” in *2003 International Conference on Multimedia and Expo. ICME’03. Proceedings (Cat. No. 03TH8698)*, vol. 1. IEEE, 2003, pp. 1–629.
- [4] S. Zhang, Z. Yang, J. Yang, and Y. Huang, “Provably secure generative linguistic steganography,” in *Findings of the Association for Computational Linguistics: ACL-IJCNLP 2021*, 2021, pp. 3046–3055.
- [5] G. Kaptchuk, T. M. Jois, M. Green, and A. D. Rubin, “Meteor: Cryptographically secure steganography for realistic distributions,” in *Proceedings of the 2021 ACM SIGSAC Conference on Computer and Communications Security*, ser. CCS ’21. New York, NY, USA: Association for Computing Machinery, 2021, p. 1529–1548.
- [6] J. Ding, K. Chen, Y. Wang, N. Zhao, W. Zhang, and N. Yu, “Discop: Provably secure steganography in practice based on “distribution copies,”” in *2023 IEEE Symposium on Security and Privacy (SP)*. IEEE Computer Society, 2023, pp. 2238–2255.
- [7] L. Xiang, W. Wu, X. Li, and C. Yang, “A linguistic steganography based on word indexing compression and candidate selection,” *Multimedia Tools and Applications*, vol. 77, pp. 28 969–28 989, 2018.
- [8] Z. Ziegler, Y. Deng, and A. M. Rush, “Neural linguistic steganography,” in *Proceedings of the 2019 Conference on Empirical Methods in Natural Language Processing and the 9th International Joint Conference on Natural Language Processing (EMNLP-IJCNLP)*, 2019, pp. 1210–1215.
- [9] J. Yang, Z. Yang, J. Zou, H. Tu, and Y. Huang, “Linguistic steganalysis toward social network,” *IEEE Transactions on Information Forensics and Security*, vol. 18, pp. 859–871, 2022.
- [10] H. Wang, Z. Yang, J. Yang, C. Chen, and Y. Huang, “Linguistic steganalysis in few-shot scenario,” *IEEE Transactions on Information Forensics and Security*, 2023.
- [11] Y. Xue, J. Wu, R. Ji, P. Zhong, J. Wen, and W. Peng, “Adaptive domain-invariant feature extraction for cross-domain linguistic steganalysis,” *IEEE Transactions on Information Forensics and Security*, 2023.
- [12] J. Bai, S. Bai, and Y. C. et al., “Qwen technical report,” *arXiv preprint arXiv:2309.16609*, 2023.
- [13] A. Q. Jiang, A. Sablayrolles, A. Mensch, C. Bamford, D. S. Chaplot, D. d. l. Casas, F. Bressand, G. Lengyel, G. Lample, L. Saulnier, et al., “Mistral 7b,” *arXiv preprint arXiv:2310.06825*, 2023.
- [14] H. Touvron, L. Martin, K. Stone, P. Albert, A. Almahairi, Y. Babaei, N. Bashlykov, S. Batra, P. Bhargava, S. Bhosale, et al., “Llama 2: Open foundation and fine-tuned chat models,” *arXiv preprint arXiv:2307.09288*, 2023.
- [15] A. Dubey, A. Jauhri, A. Pandey, A. Kadian, A. Al-Dahle, A. Letman, A. Mathur, A. Schelten, A. Yang, A. Fan, et al., “The llama 3 herd of models,” *arXiv preprint arXiv:2407.21783*, 2024.
- [16] A. L. Maas, R. E. Daly, P. T. Pham, D. Huang, A. Ng, and C. Potts, “Learning word vectors for sentiment analysis,” in *Annual Meeting of the Association for Computational Linguistics*, 2011.
- [17] Z. Yang, Y. Huang, and Y. Zhang, “Ts-csw: Text steganalysis and hidden capacity estimation based on convolutional sliding windows,” *Multimedia Tools and Applications*, vol. 79, pp. 18 293–18 316, 2020.
- [18] Z. Yang, K. Wang, J. Li, Y. Huang, and Y.-J. Zhang, “Ts-rnn: text steganalysis based on recurrent neural networks,” *IEEE Signal Processing Letters*, vol. 26, no. 12, pp. 1743–1747, 2019.
- [19] Y. Niu, J. Wen, P. Zhong, and Y. Xue, “A hybrid r-bilstm-c neural network based text steganalysis,” *IEEE Signal Processing Letters*, vol. 26, no. 12, pp. 1907–1911, 2019.
- [20] ayaan04. Shakespere dataset. Huggingface. [Online]. Available: <https://hf.com/datasets/ayaan04/shakespeare-text>
- [21] Y. Bai, A. Jones, K. Ndousse, A. Askell, A. Chen, N. DasSarma, D. Drain, S. Fort, D. Ganguli, T. Henighan, et al., “Training a helpful and harmless assistant with reinforcement learning from human feedback,” *arXiv preprint arXiv:2204.05862*, 2022.
- [22] G. Liao, J. Yang, K. Pang, and Y. Huang, “Co-stega: Collaborative linguistic steganography for the low capacity challenge in social media,” in *Proceedings of the 2024 ACM Workshop on Information Hiding and Multimedia Security*, 2024, pp. 7–12.
- [23] K. Pang, M. Bai, J. Yang, H. Wang, M. Jiang, and Y. Huang, “Fremax: A simple method towards truly secure generative linguistic steganography,” in *ICASSP 2024-IEEE International Conference on Acoustics, Speech and Signal Processing (ICASSP)*. IEEE, 2024, pp. 4755–4759.
- [24] J. Shen, H. Ji, and J. Han, “Near-imperceptible neural linguistic steganography via self-adjusting arithmetic coding,” in *Proceedings of the 2020 Conference on Empirical Methods in Natural Language Processing (EMNLP)*, 2020, pp. 303–313.
- [25] N. J. Hopper, *Toward a theory of Steganography*. Carnegie Mellon University, 2004.
- [26] T. Fang, M. Jaggi, and K. Argyraki, “Generating steganographic text with LSTMs,” in *Proceedings of ACL 2017, Student Research Workshop*. A. Ettinger, S. Gella, M. Labeau, C. O. Alm, M. Carpuat, and M. Dredze, Eds. Vancouver, Canada: Association for Computational Linguistics, July 2017, pp. 100–106.
- [27] Z. Yang, X. Guo, Z. Chen, Y. Huang, and Y.-J. Zhang, “Rnn-stega: Linguistic steganography based on recurrent neural networks,” *IEEE Transactions on Information Forensics and Security*, 2018.
- [28] F. Dai and Z. Cai, “Towards near-imperceptible steganographic text,” in *Proceedings of the 57th Annual Meeting of the Association for Computational Linguistics*. Florence, Italy: Association for Computational Linguistics, July 2019, pp. 4303–4308.
- [29] Y. Xue, L. Kong, W. Peng, P. Zhong, and J. Wen, “An effective linguistic steganalysis framework based on hierarchical mutual learning,” *Information Sciences*, vol. 586, pp. 140–154, 2022.
- [30] B. LeBrun, A. Sordani, and T. J. O’Donnell, “Evaluating distributional distortion in neural language modeling,” in *International Conference on Learning Representations*, 2022.
- [31] H. Ji, P. Ke, Z. Hu, R. Zhang, and M. Huang, “Tailoring language generation models under total variation distance,” in *The Eleventh International Conference on Learning Representations*, 2023.
- [32] S. Zhang, S. Wu, O. Irsoy, S. Lu, M. Bansal, M. Dredze, and D. Rosenberg, “Mixce: Training autoregressive language models by mixing forward and reverse cross-entropies,” in *The 61st Annual Meeting Of The Association For Computational Linguistics*, 2023.
- [33] E. Ilia and W. Aziz, “Predict the next word: <humans exhibit uncertainty in this task and language models _____>,” in *Proceedings of the 18th Conference of the European Chapter of the Association for Computational Linguistics (Volume 2: Short Papers)*. St. Julian’s, Malta: Association for Computational Linguistics, Mar. 2024, pp. 234–255.
- [34] C. Manning and H. Schütze, *Foundations of statistical natural language processing*. MIT press, 1999.
- [35] Y. Wang, I. Wood, S. Wan, M. Dras, and M. Johnson, “Mention flags (MF): Constraining transformer-based text generators,” in *Proceedings of the 59th Annual Meeting of the Association for Computational Linguistics and the 11th International*

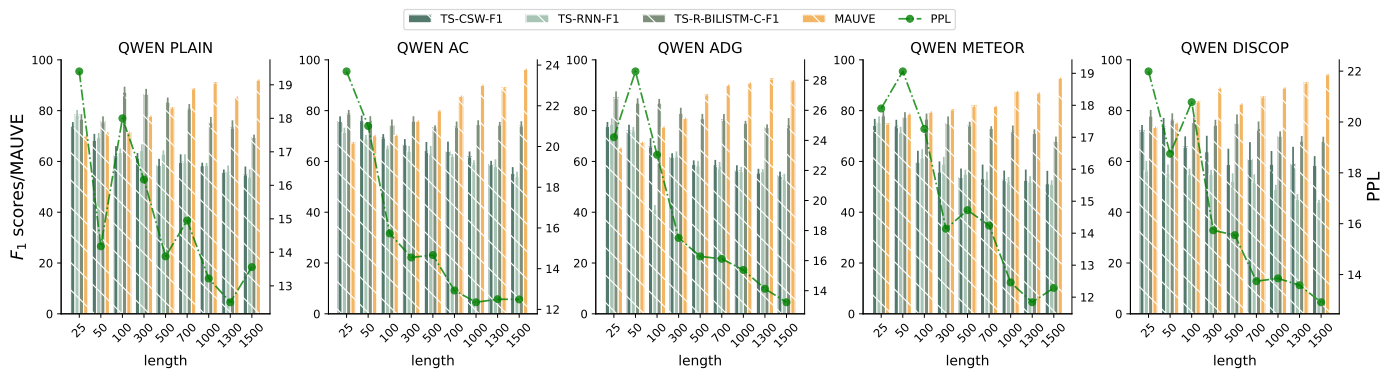


Fig. 12. The effect of the number of target domain texts used for alignment on QWEN2 for XHS.

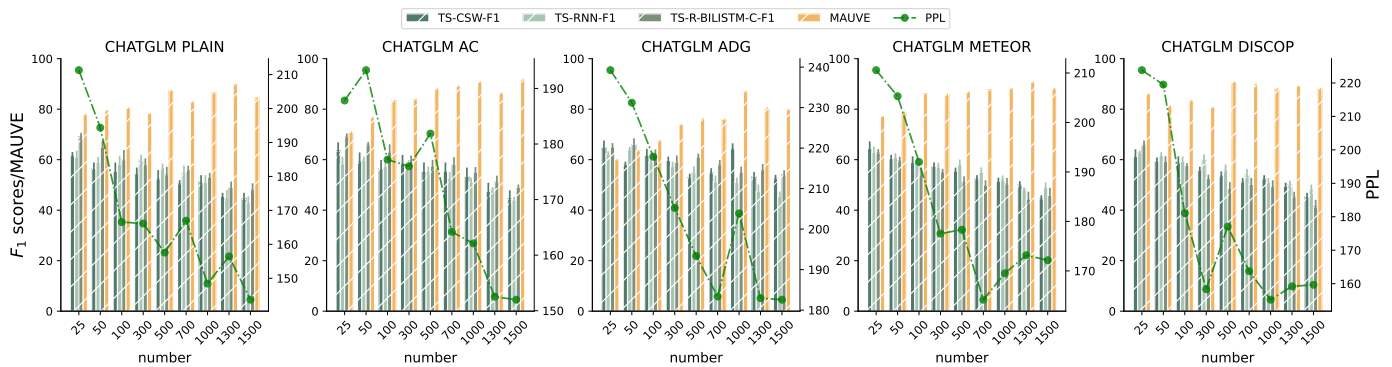


Fig. 13. The effect of the number of target domain texts used for alignment on CHATGLM for XHS.

Joint Conference on Natural Language Processing (Volume 1: Long Papers), C. Zong, F. Xia, W. Li, and R. Navigli, Eds. Online: Association for Computational Linguistics, Aug. 2021, pp. 103–113.

- [36] K. Arora, K. Shuster, S. Sukhbaatar, and J. Weston, “Director: Generator-classifiers for supervised language modeling,” in *Proceedings of the 2nd Conference of the Asia-Pacific Chapter of the Association for Computational Linguistics and the 12th International Joint Conference on Natural Language Processing (Volume 1: Long Papers)*. Online only: Association for Computational Linguistics, Nov. 2022, pp. 512–526.
- [37] H. Zhang and D. Song, “Discup: Discriminator cooperative unlikelyhood prompt-tuning for controllable text generation,” in *Proceedings of the 2022 Conference on Empirical Methods in Natural Language Processing*. Association for Computational Linguistics, 2022, pp. 3392–3406.
- [38] X. L. Li and P. Liang, “Prefix-tuning: Optimizing continuous prompts for generation,” in *Proceedings of the 59th Annual Meeting of the Association for Computational Linguistics and the 11th International Joint Conference on Natural Language Processing*, 2021, pp. 4582–4597.
- [39] T. Shin, Y. Razeghi, R. L. Logan IV, E. Wallace, and S. Singh, “Autoprompt: Eliciting knowledge from language models with automatically generated prompts,” in *Proceedings of the 2020 Conference on Empirical Methods in Natural Language Processing (EMNLP)*. Association for Computational Linguistics, 2020.
- [40] W. Zhou, Y. E. Jiang, E. Wilcox, R. Cotterell, and M. Sachan, “Controlled text generation with natural language instructions,” in *International Conference on Machine Learning*. PMLR, 2023, pp. 42 602–42 613.
- [41] E. J. Hu, Y. Shen, P. Wallis, Z. Allen-Zhu, Y. Li, S. Wang, L. Wang, and W. Chen, “LoRA: Low-rank adaptation of large language models,” in *International Conference on Learning Representations*, 2022.
- [42] O. L. et al., “Training language models to follow instructions with human feedback,” in *Proceedings of the 36th International Conference on Neural Information Processing Systems*, 2024.
- [43] G. Qin and J. Eisner, “Learning how to ask: Querying lms with mixtures of soft prompts,” in *Proceedings of the 2021 Conference of the North American Chapter of the Association for Computational Linguistics: Human Language Technologies (NAACL-HLT)*, 2021.
- [44] R. Yang, X. Pan, F. Luo, S. Qiu, H. Zhong, D. Yu, and J. Chen, “Rewards-in-context: Multi-objective alignment of foundation models with dynamic preference adjustment,” in *Proceedings of the 41st International Conference on Machine Learning*, ser. Proceedings of Machine Learning Research, vol. 235. PMLR, 21–27 Jul 2024, pp. 56 276–56 297.
- [45] Y. Zhong, C. Ma, X. Zhang, Z. Yang, Q. Zhang, S. Qi, and Y. Yang, “Panacea: Pareto alignment via preference adaptation for llms,” *Advances in Neural Information Processing Systems*, vol. 36, 2024.
- [46] S. Dathathri, A. Madotto, J. Lan, J. Hung, E. Frank, P. Molino, J. Yosinski, and R. Liu, “Plug and play language models: A simple approach to controlled text generation,” in *International Conference on Learning Representations*, 2019.
- [47] B. Krause, A. D. Gotmare, B. McCann, N. S. Keskar, S. R. Joty, R. Socher, and N. Rajani, “Gedi: Generative discriminator guided sequence generation,” in *Conference on Empirical Methods in Natural Language Processing*, 2020.
- [48] K. Yang and D. Klein, “FUDGE: controlled text generation with future discriminators,” in *Proceedings of the 2021 Conference of the North American Chapter of the Association for Computational Linguistics: Human Language Technologies, NAACL-HLT 2021, Online, June 6-11, 2021*. Association for Computational Linguistics, 2021, pp. 3511–3535.
- [49] C. Chen, J. Yang, Y. Gao, H. Wang, and Y. Huang, “Minimizing distortion in steganography via adaptive language model tuning,” in *International Conference on Neural Information Processing*. Springer, 2023, pp. 571–584.
- [50] C. E. Shannon, “A mathematical theory of communication,” *The Bell system technical journal*, vol. 27, no. 3, pp. 379–423, 1948.
- [51] Y. B. et al., “Coig-cqia: Quality is all you need for chinese instruction fine-tuning,” *CoRR*, vol. abs/2403.18058, 2024.
- [52] Z. Du, Y. Qian, X. Liu, M. Ding, J. Qiu, Z. Yang, and J. Tang, “Glm: General language model pretraining with autoregressive blank infilling,” in *Proceedings of the 60th Annual Meeting of the Association for Computational Linguistics (Volume 1: Long Papers)*, 2022, pp. 320–335.
- [53] K. Pillutla, S. Swamyamdipta, R. Zellers, J. Thickstun, S. Welleck, Y. Choi, and Z. Harchaoui, “Mauve: Measuring the gap between neural text and human text using divergence frontiers,” *Advances in Neural Information Processing Systems*, vol. 34, pp. 4816–4828, 2021.
- [54] Y. Niu, J. Wen, P. Zhong, and Y. Xue, “A hybrid r-bilstm-c neural network based text steganalysis,” *IEEE Signal Processing Letters*, vol. 26, no. 12, pp. 1907–1911, 2019.
- [55] P. Liu, W. Yuan, J. Fu, Z. Jiang, H. Hayashi, and G. Neubig, “Pre-train, prompt, and predict: A systematic survey of prompting methods in natural language processing,” *ACM Computing Surveys*, vol. 55, no. 9, jan 2023.
- [56] G. Bao, Y. Zhao, Z. Teng, L. Yang, and Y. Zhang, “Fast-detectept: Efficient zero-shot detection of machine-generated text via conditional probability curvature,” in *ICLR*, 2024.
- [57] K. Lin, Y. Luo, Z. Zhang, and L. Ping, “Zero-shot generative linguistic steganography,” in *Proceedings of the 2024 Conference of the North American Chapter of the Association for Computational Linguistics*, K. Duh, H. Gomez, and S. Bethard, Eds. Association for Computational Linguistics, June 2024, pp. 5168–5182.
- [58] J. Bergstra and Y. Bengio, “Random search for hyper-parameter optimization,” *Journal of Machine Learning Research*, vol. 13, no. 10, pp. 281–305, 2012.
- [59] J. Snoek, H. Larochelle, and R. P. Adams, “Practical bayesian optimization of machine learning algorithms,” *Advances in neural information processing systems*, vol. 25, 2012.

VI. APPENDIX

A. KL divergence of the non-distribution-preserving algorithm

If the noise introduced by steganography is significant—specifically, for many non-distribution-preserving algorithms, where we assume $\forall \epsilon(x)$ exceeds a certain threshold $\delta(x)$ —then for each value x in distribution, we have:

$$D_{KL}(p_{\mathcal{E}}(x), p_{\mathcal{S}}(x)) = \sum_x p_{\mathcal{E}}(x) \left[\log \frac{p_{\mathcal{E}}(x)}{p_{\mathcal{M}}(x)} - \log \left(1 + \frac{\epsilon(x)}{p_{\mathcal{M}}(x)} \right) \right] \quad (23)$$

The latter term follows the formula 24 with a detailed proof 1.

$$\log \left(1 + \frac{\epsilon(x)}{p_{\mathcal{M}}(x)} \right) = \log \left(1 + \frac{p_{\mathcal{S}}(x) - p_{\mathcal{M}}(x)}{p_{\mathcal{M}}(x)} \right) \leq \frac{1 - 2\delta(x)}{\delta(x)} \quad (24)$$

This gap consists of the model-environment distribution difference and steganography noise.

$$D_{KL}(p_{\mathcal{E}}, p_{\mathcal{S}}) \geq D_{KL}(p_{\mathcal{E}}, p_{\mathcal{M}}) - \sum_x \frac{1 - 2\delta(x)}{\delta(x)} p_{\mathcal{E}}(x) \quad (25)$$

Improving the alignment between the language model distribution and the cover text distribution still remains crucial for enhancing imperceptibility.

Lemma 1. *If $\delta \leq p, q \leq 1 - \delta$ and $|p - q| \geq \delta$, then the following holds:*

$$\left| \log \left(1 + \frac{q - p}{p} \right) \right| \leq \frac{1 - 2\delta}{\delta}.$$

By symmetry, the same inequality applies to $\left| \log \left(1 - \frac{q - p}{1 - p} \right) \right|$.

Proof: Define $z = 1 + \frac{q - p}{p}$. If $q > p$, then z is positive and achieves its maximum when $p = \delta$ and $q = 1 - \delta$, or when $q = \delta$. In this case, we have:

$$z = \log \left(1 - \frac{1 - 2\delta}{1 - \delta} \right) \leq \frac{1 - 2\delta}{\delta}.$$

If $q < p$, then z is negative and minimized when $p = 1 - \delta$ and $q = \delta$. In this situation, we obtain:

$$z = \log \left(1 - \frac{1 - 2\delta}{1 - \delta} \right) \geq \frac{-\left(\frac{1 - 2\delta}{1 - \delta}\right)}{1 - \frac{1 - 2\delta}{1 - \delta}} = -\frac{1 - 2\delta}{\delta}.$$

B. Experiment details

We present the basic statistical results of the human corpus and examples of the prompts used in the experiment. The corpus statistics are shown in Table IX, while the prompts for different datasets are listed in Table X. The fine-tuning details in the compatibility analysis are show in Table XI. The prompt used in the zero-shot setting in the compatibility analysis is:

Prompt Templates Used in Zero-shot setting

[SYSTEM PROMPT]: You are skilled at mimicking the XHS style. Please generate an XHS post according to the following requirements: use conversational short sentences, appropriate line breaks, and insert 1–2 related emojis per paragraph. Naturally embed keywords and tags.

[USER QUERY]: Topic.

The prompt used in the few-shot setting in the compatibility analysis is:

Prompt Templates Used in ZGLS [57]

[SYSTEM PROMPT]: You are an expert at mimicking the language style of others. Users will input sentences from a given corpus. You have to create **ONE** similar sentence.

[USER QUERY]: Write a similar one to the context.

Example sentence 1.

Example sentence 2.

TABLE IX
STATISTICS OF HUMAN CORPUS. WE USED QWEN2 TO COMPUTE THE AVERAGE VALUES OF THESE METRICS

Corpus	IMDB	XHS	Shakespeare
Language	English	Chinese	English
Size	1,054,802	50,000	18,395
Tokens	25,809,893	588,334	241,212

TABLE X
PROMPT EXAMPLE

Dataset	Prompt
IMDB	Generate a user review for the movie in one sentence, without including the movie title.
XHS	你是一名小红书博主，写一篇以“对于我这个老减脂人咖啡实在太重要了”为题目的小红书。(You are a XHS blogger. Write a post titled "For Someone Like Me Who's Been Cutting Fat for a Long Time, Coffee Is Just Too Important.)
SHAKESPEARE	You are a model which converts all of my input normal text into Shakespearean styled text. My input text is: He loves Caesar best, but he also loves Antony.

C. Case Study

Tables XIII, XIV, and XV present the results for human references, stego texts generated without FreStega, and stego texts generated with FreStega, in the styles of IMDB, Shakespeare, and XHS, respectively. The results demonstrate that FreStega helps align stego texts with real cover texts in the target domain, enhancing the stego texts with a more pronounced target domain style (e.g., emojis and tags in XHS, common user abbreviations in IMDB, and Shakespearean expressions). This alignment improves the imperceptibility of stego texts in real-world scenarios.

Base model	QWEN2-7B + LoRA
Batch size	1
Max learning rate	2e-5
Training data	1000
Trainable params	40,370,176
Cutoff length	1024
Optimizer	Adam
Epochs	3
LoRA rank	16
LoRA alpha	32
LoRA dropout	0.05

TABLE XI
FINE-TUNING HYPERPARAMETERS

D. Ablation Study

We also conducted ablation experiments to compare and validate the effects of sequential temperature adjustment and spatial adjustment of FreStega. As detailed in Table XII, due to space limitations, we only present the results for DISCOP on QWEN2, as DISCOP is the latest and performance-well distribution-preserving steganography algorithm. It is evident that either sequential temperature adjustment or spatial adjustment alone can effectively align with the target corpus and provide benefits. Spatial alignment better matches the target domain style, providing greater benefits in terms of the MAUVE metric. Sequential alignment enhances the diversity of the generated text while also increasing the embedding capacity. Furthermore, combining sequential temperature adjustment with Spatial Adjustment can lead to a more pronounced convergence toward the desired alignment and better security. In our method, Sequential Adjustment is performed before Spatial Adjustment. As shown in Table XII, we also tested reversing this order. While applying Spatial Adjustment first can still improve alignment, the gains are less pronounced. This is because Sequential Adjustment provides broader temperature regulation, whereas Spatial Adjustment focuses on finer, token-level alignment tailored to the target domain.

TABLE XII

ABLATION EXPERIMENT OF QWEN2 DISCOP ON THREE DATASETS: SA (SPATIAL ALIGNMENT), TA (SEQUENTIAL ALIGNMENT), SA→TA (SPATIAL FOLLOWED BY SEQUENTIAL ALIGNMENT), AND TA→SA (OUR METHOD).

Dataset	XHS					IMDB					Shakespeare				
	PPL	Entro.	Dist3	MAUVE	CSW-F ₁	PPL	Entro.	Dist3	MAUVE	CSW-F ₁	PPL	Entro.	Dist3	MAUVE	CSW-F ₁
Vanilla	11.02	2.13	0.78	74.63	87.81% _{2.15%}	2.34	0.73	0.13	0.53	85.36% _{4.32%}	3.07	1.36	0.40	0.96	80.84% _{1.00%}
SA	10.93	2.05	0.81	86.32	67.48% _{2.32%}	2.18	0.71	0.32	1.42	73.82% _{1.38%}	2.86	1.25	0.49	6.82	61.28% _{1.22%}
TA	13.57	2.25	0.84	85.12	66.36% _{1.92%}	3.28	0.82	0.36	1.29	74.73% _{1.46%}	3.25	1.81	0.56	5.12	58.67% _{1.90%}
SA→TA	12.81	2.20	0.83	90.18	60.07% _{3.22%}	3.15	0.80	0.35	1.45	74.82% _{2.50%}	3.22	1.51	0.53	7.38	57.99% _{1.28%}
TA→SA	11.74	2.17	0.81	92.47	55.56% _{2.90%}	2.42	0.76	0.33	1.76	72.13% _{1.12%}	3.18	1.39	0.52	8.19	55.60% _{2.77%}

TABLE XIII
EXAMPLES IN IMDB USING QWEN2 DISCOP

Method	Generated Texts
Human	the special fx are cheesy and the singing and dancing is mediocre
w/o FreStega	A captivating, suspenseful film that masterfully combines thrilling action sequences with intricate plot twists and compelling characters.
w. FreStega	Despite a weak script, the stunning fx made it worth watching.

TABLE XIV
EXAMPLES IN SHAKESPEARE USING QWEN2 DISCOP

Method	Generated Texts
Prompt	You are a model that converts all of my input normal text into Shakespearean styled text. My input text is: I have half a mind to hit you before you speak again.
Human	I have a mind to strike thee ere thou speak'st.
w/o FreStega	Thy next word might provoke mine hand, anon.
w. FreStega	Thy next word might provoke mine hand to strike, methinks.

TABLE XV
EXAMPLES IN XHS WITH QWEN2 DISCOP

Method	Generated Texts
Prompt	请以小红书博主的口吻，以挑战15天马甲线第13天为标题写一篇小红书分享
Human	嘻嘻，好开心这个算不算挑战成功🥳今天我来说几点一：我不是专业健身教练，我动作不精准，甚至不规范，请你们谅解！毕竟我也是跟着运动教程去做的！我只是坚持了，[害羞R][害羞R]所以我要感谢你们的喜欢和包容，你们相信我，坚持下来一定会有收获🙏二：一定要先减脂，先减肥，因为瘦下来塑型会让你效果更快更明显👉三：不用纠结动作，哪怕就是十个动作每天重复练，你照样可以有马甲线，而且肯定比我更厉害👉四：发力点，一定要腹部发力，收紧腹部，腹部带动腿部，身体！记住哈，发力点对了效果快👉五：我没有控制饮食，因为我已经瘦下来了，不需要控制饮食，胖的人需要控制！🍎最后，你们一定要加油。想要效果快，每天多练，我就是为了让大家监督我，所以严格要求自己的！👊
w/o FreStega	标题：👉 15天马甲线挑战：Days 1-13小记:坚持就是胜利！宝贝们！今天是马甲线挑战的第13天了！简直不敢相信时间过得这么快！（#马甲线挑战#15天挑战）这13天中，我感到了自己的变化，从一开始的困惑和犹豫到现在的自信和坚持。👉这距离第一次开始计时已经过了快两周，开始我只觉得这个计划好遥远。但现在，我每天醒来都充满期待，期待自己今天的进步和挑战更强大的自己。每一天的运动都是对自己的一次小挑战：腹部训练、瑜伽、深蹲、仰卧起坐.....每一个动作虽然简单，但汇聚在一起就是改变。我开始留意肚皮在收缩时的感觉，那种奇妙的奇迹感让我每次都会露出满足的微笑。失砂の岁月，魔界、鹤烽，而这不仅仅是一种外观的改变，它也是心态的转变。我知道，真正的改变是从心中开始的。每天看着镜子中的自己，我变得更加自信，挑战身体极限。
w. FreStega	标题：👉 15天马甲线倒计时第13天：身体的小秘密，只对坚持的人展示！👉正文：大家好！亲爱的小伙伴们👉我是你们的健身小伙伴，今天继续和大家分享我的马甲线挑战进度啦！👉第13天，我已经感觉自己和马甲线之间的距离一天比一天近！👉每次做起来腹部动作时，总能感觉到肌肉在暗示我：你越来越接近目标了呢👉这13天的经历，让我深刻认识到坚持的力量！力量远远超出了我的想象。每一天的付出都在预扣着未来的好身材，我得珍惜每一次的汗水👉。为了今天的效果，昨晚的晚餐我选择了清淡的沙拉搭配鸡胸肉，今天早餐也是高蛋白的蛋白饼，都是为了给肌肉更好的恢复和生长环境。👉营养永远是健身的伴侣，这13天我学会了更多关于饮食的知识！👉摄入要讲究，摄入要健康！明天就是这15天挑战的最后两天啦！激动又紧张，不过我知道成功要靠自己一步一步走过去，我不会放弃的！👉 #练出腹肌马甲线#瘦全身